Overexpression of Sly41 suppresses COPII vesicle–tethering deficiencies by elevating intracellular calcium levels

Indrani Mukherjee and Charles Barlowe*
Department of Biochemistry, Geisel School of Medicine at Dartmouth, Hanover, NH 03755

ABSTRACT *SLY41* was identified as a multicopy suppressor of loss of Ypt1, a Rab GTPase essential for COPII vesicle tethering at the Golgi complex. *SLY41* encodes a polytopic membrane protein with homology to a class of solute transporter proteins, but how overexpression suppresses vesicle-tethering deficiencies is not known. Here we show that Sly41 is efficiently packaged into COPII vesicles and actively cycles between the ER and Golgi compartments. *SLY41* displays synthetic negative genetic interactions with *PMR1*, which encodes the major Golgi-localized Ca^{2+}/Mn^{2+} transporter and suggests that Sly41 influences cellular Ca^{2+} and Mn^{2+} homeostasis. Experiments using the calcium probe aequorin to measure intracellular Ca^{2+} concentrations in live cells reveal that Sly41 overexpression significantly increases cytosolic calcium levels. Although specific substrates of the Sly41 transporter were not identified, our findings indicate that localized overexpression of Sly41 to the early secretory pathway elevates cytosolic calcium levels to suppress vesicle-tethering mutants. In vitro SNARE cross-linking assays were used to directly monitor the influence of Ca^{2+} on tethering and fusion of COPII vesicles with Golgi membranes. Strikingly, calcium at suppressive concentrations stimulated SNARE-dependent membrane fusion when vesicle-tethering activity was reduced. These results show that calcium positively regulates the SNARE-dependent fusion stage of ER–Golgi transport.

INTRODUCTION

The secretory pathway is responsible for delivery of proteins and lipids from their site of synthesis at the endoplasmic reticulum (ER) to endocytic and exocytic membrane compartments. Bidirectional vesicular transport between the ER and Golgi is a key step in the transport of secretory cargo to their proper cellular locations (Lee *et al.*, 2004). Structural, genetic, biochemical, and morphological studies across multiple cell types have provided a wealth of informa-

tion on the protein machinery involved in vesicular transport between the ER and Golgi compartments (Brandizzi and Barlowe, 2013). In general outline, the coat protein complex II (COPII) selects cargo into transport intermediates at the ER for forward transport to Golgi membranes, whereas the coat protein complex I (COPI) forms retrograde-directed vesicles to recycle transport machinery to the ER. Compartment-specific tethering factors target these transport vesicles to their correct acceptor sites for soluble *N*-ethylmaleimide–sensitive factor attachment protein receptor (SNARE) protein–dependent membrane fusion. Although an outline for ER–Golgi trafficking is known, underlying mechanisms and regulation of distinct transport stages are not well understood.

Through biochemical and genetic studies in yeast, fusion of COPII vesicles with *cis*-Golgi membranes can be separated into distinct stages of vesicle tethering and fusion (Rexach and Schekman, 1991; Cao *et al.*, 1998; Sacher *et al.*, 2001). COPII vesicle tethering requires the Rab GTPase Ypt1 (Schmitt *et al.*, 1988; Segev *et al.*, 1988), the extended coil-coiled domain protein Uso1 (Nakajima *et al.*, 1991), and the multisubunit TRAPPI complex (Sacher *et al.*, 2001). Fusion of tethered vesicles depends on the SNARE proteins

Sed5, Bos1, Bet1, and Sec22, which are assembled into four-helix *trans*-SNARE complexes through the action of Sly1 (Newman *et al.*, 1990; Hardwick and Pelham, 1992; Sogaard *et al.*, 1994; Cao and Barlowe, 2000). Sly1 is a member of the Sec1/Munc18 (SM) family of proteins and catalyzes assembly of *trans*-SNARE complexes through direct interactions (Peng and Gallwitz, 2002; Demircioglu *et al.*, 2014; Lobingier *et al.*, 2014). Major insights into the identification and sequential order of these membrane-tethering and fusion factors came out of genetic screens for suppressors of loss of Ypt1, termed the *SLY* genes (Dascher *et al.*, 1991; Ossig *et al.*, 1991). In fact, Sly1 was initially identified as a gain-of-function *SLY1-20* chromosomal allele, which contains a single point mutation that bypasses the need for Ypt1 activity. Of interest, *SLY1-20* suppresses other deficiencies in vesicle-tethering activities, in accord with a role for Sly1 function in stages after Ypt1- and Uso1-dependent tethering (Sapperstein *et al.*, 1996; Cao *et al.*, 1998). Additional *SLY* suppressors include multicopy plasmids containing the genes *SLY2/SEC22* and *SLY12/BET1*, which encode the very SNARE proteins that catalyze fusion of COPII vesicles with Golgi membranes. These findings support a model in which *SLY* genes activate the SNARE-dependent membrane fusion stage to compensate for inefficient vesicle tethering.

SLY41 was also identified as a multicopy suppressor in the screen for loss of *YPT1*. *SLY41* encodes a 453–amino acid multispanning membrane protein that shares sequence homology to the SLC35 family of solute carriers, which includes nucleotide sugar transporters (Dascher *et al.*, 1991; Mi *et al.*, 2013). The mechanism of suppression by *SLY41* is unknown. In this study, we identify Sly41 as a COPII vesicle protein that traffics between the ER and Golgi. Whereas the cellular function of Sly41 remains unclear, our results show that Sly41 overexpression suppresses the loss of *YPT1* by elevating cytosolic levels of calcium in the cell. Several lines of evidence indicate that calcium plays a role in regulation of membrane trafficking through the early secretory pathway (Beckers and Balch, 1989; Rexach and Schekman, 1991; Porat and Elazar, 2000; Chen *et al.*, 2002; Bentley *et al.*, 2010; Helm *et al.*, 2014). However, calcium does not appear to be absolutely required for SNARE-dependent membrane fusion (Parlati *et al.*, 2000; Flanagan and Barlowe, 2006). Calcium is also known to have significant effects on the properties of charged phospholipid bilayers, which in turn influence membrane fusion (Pedersen *et al.*, 2006; Tarafdar *et al.*, 2012; Mao *et al.*, 2013). The mechanism(s) by which calcium affects membrane trafficking in the early secretory pathway are not known. Our present in vivo and cell-free studies show that specific calcium levels can stimulate the SNARE-dependent fusion stage of COPII vesicles with *cis*-Golgi membranes.

RESULTS

Sly41 is an integral membrane protein with cytosolic N- and C-termini

Comprehensive proteomic analyses of purified COPII vesicles identified Sly41 as a constituent of these vesicles (Margulis *et al.*, 2016). On the basis of previous work showing that overexpressed *SLY41* suppressed COPII vesicle–tethering deficiencies (Dascher *et al.*, 1991), we investigated how this vesicle protein could influence fusion of COPII vesicles with *cis*-Golgi membranes. Sequence analysis predicts that Sly41 is an integral membrane protein possessing eight transmembrane domains (von Heijne, 1992). Sly41 belongs to the solute carrier (SLC) family of proteins, which comprises 55 gene families and >300 putatively functional protein-coding genes (He *et al.*, 2009). Sly41 bears 24% identity to its human homologue, SLC35E1, which is also of unknown function. Apart from this, Sly41

also bears various degrees of similarity to other known transporters of the SLC family in yeast, such as Ymd8 (involved in UDP-glucose transport), Yea4 (UDP-*N*-acetylglucosamine transporter), and Vrg4 (GDP-mannose transporter) as reported (De Hertogh *et al.*, 2002; He *et al.*, 2009; Hoglund *et al.*, 2011). Multipass transmembrane proteins can exist in a few different topologies, and to gain a better understanding of domain arrangements in Sly41, we conducted protease protection experiments to test the location of the N-terminus and C-terminus. Polyclonal antiserum raised against the N-terminal 112 amino acid residues was generated and recognized a 41-kDa protein by immunoblot of whole cells that was not detected in a *sly41Δ* strain. A C-terminal epitope-tagged Sly41HA version was also analyzed to probe the orientation of the C-terminus.

Protease protection assays were carried out using ER microsomes prepared from wild-type and Sly41HA strains. Treatment of the microsomes with trypsin in the absence or presence of detergent can be used to determine cytosolic accessibility of the N- and C-termini of Sly41. Trypsin treatment digested virtually all of the detectable Sly41 N-terminus and hemagglutinin (HA)-tagged C-terminus (Figure 1). As controls for membrane integrity and trypsin activity in these experiments, Erv41, a transmembrane protein with relatively short cytosolic segments and a large protected luminal domain, and the cytosol-facing SNARE protein Bos1 were monitored. On protease treatment, Erv41 shifted to a protease-protected species of the expected size, whereas Bos1 was fully digested (Otte and Barlowe, 2002). Addition of trypsin in the presence of detergent caused digestion of all proteins examined. Collectively these observations indicate that the N- and C-termini of Sly41 are cytosolically exposed, consistent with the proposed topology model. Using the Sly41-specific antiserum, we next characterized the distribution and trafficking of Sly41.

Sly41 cycles between the ER and Golgi compartments by means of COPII vesicles

Integral membrane COPII vesicle proteins could be components of the ER/Golgi transport machinery or secretory proteins en route to their final cellular location. Of interest, C-terminally green fluorescent protein (GFP)–tagged Sly41 was localized to ER membranes (Huh *et al.*, 2003). However, genetic studies showed that Sly41 displays genetic interactions with proteins that function at both the ER and the Golgi complex (Dascher *et al.*, 1991; Ossig *et al.*, 1991; Kito *et al.*, 1996). These results suggest that Sly41 might cycle between the ER and Golgi compartments, but fusing GFP to the C-terminus impedes trafficking. To investigate this hypothesis, we prepared cell lysates from wild-type and Sly41 overexpressor strains to monitor the subcellular localization of Sly41 on sucrose gradients. In both cases, Sly41 sedimented in two peaks, one that coincided with the Golgi marker Och1 and one with the ER marker Yet3 (Figure 2, A and B). We observed that overexpression of *SLY41* from a 2μ plasmid increased Sly41 levels ~10-fold (Supplemental Figure S1). These results indicate that overexpression of Sly41 to levels that suppress tethering mutants does not result in mislocalization of the protein but instead a continued distribution between the ER and Golgi compartments. Immunofluorescence microscopy confirmed a similar distribution of endogenous and overexpressed Sly41 in cells. Here a punctate Golgi-like pattern was observed in both wild-type and Sly41 overexpressor strains (Supplemental Figure S2). The observed subcellular distribution of Sly41 was comparable to other vesicle proteins that cycle between the ER and Golgi compartments (Schröder *et al.*, 1995; Cao and Barlowe, 2000; Otte and Barlowe, 2002; Heidtman *et al.*, 2005).
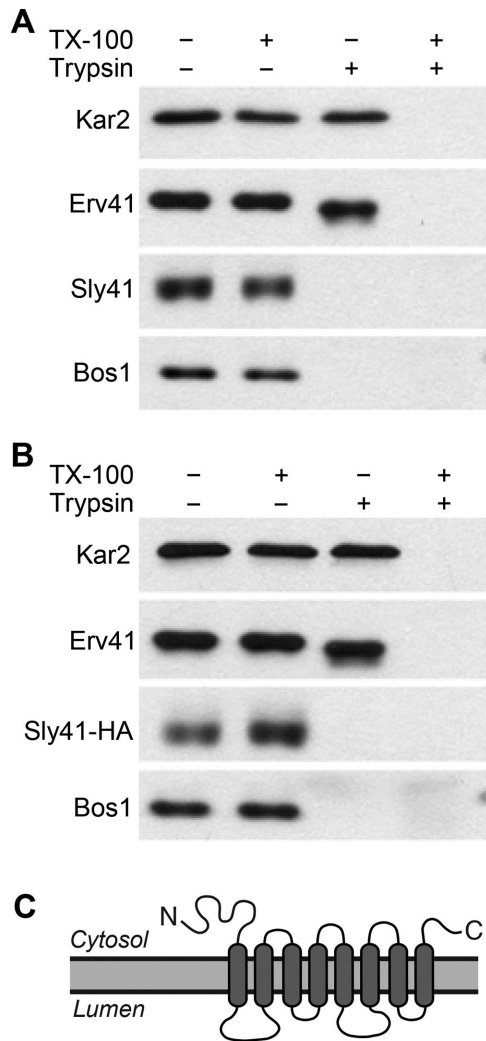
FIGURE 1: Membrane topology of Sly41. (A) Sly41 N-terminus is exposed to the cytosol. Microsomes from wild-type (CBY740) cells were treated with buffer alone, 1% Triton X-100 (TX-100), trypsin, or both Triton X-100 and trypsin. Samples were resolved on a polyacrylamide gel and blotted for Kar2 (a lumenal ER protein), Bos1 (a cytosolically exposed membrane protein), and Erv41 (membrane protein with partially exposed cytosolic N- and C-termini that undergoes an increase in electrophoretic mobility upon trypsin treatment). Sly41 was detected using polyclonal antisera specific to the N-terminus. (B) The C-terminal tail of Sly41 is cytosolically exposed. Microsomes from the *SLY41-3HA* (CBY3059) strain were treated with buffer alone, 1% Triton X-100 (TX-100), trypsin or both Triton X-100 and trypsin. Samples were immunoblotted as in A, except that Sly41-HA was detected using HA-specific monoclonal antibody. (C) Proposed topology model for Sly41, placing the N- and C-termini in the cytoplasm with eight transmembrane segments based on hydropathy plots.

FIGURE 2: Sly41 cycles between the ER and Golgi under both endogenous and overexpression conditions. Sucrose gradient fractionation of lysates from (A) wild-type (CBY80) and (B) 2μ *SLY41* (CBY3346) strains on an 18–60% density gradient. After centrifugation, fractions were collected from the top of the gradient and analyzed by immunoblot. Relative levels of Och1 (Golgi marker), Sec61 (ER marker), and Sly41 in each fraction were quantified by densitometry of immunoblots. (C) Blocking ER export in the *sec12-4* strain causes Sly41 to accumulate in the ER fraction (P13). Sec22 and Erv41, proteins that cycle between the ER and Golgi, also shift to the ER fraction. The first four lanes compare wild-type (RSY248) with *sec12-4* (RSY263) cells, and the last four lanes compare wild-type (CBY740) with *sly41Δ* (CBY3087) cells.

To test dynamic cycling of Sly41 in vivo, we analyzed the distribution of Sly41 after a *sec12-4* section block. On shifting a *sec12-4* strain to the restrictive temperature, export from the ER is blocked, and proteins that cycle between the ER and Golgi compartments accumulate in the ER (Schröder *et al.*, 1995). Wild-type and *sec12-4* cells in log-phase growth were shifted to the restrictive temperature and membrane organelles resolved by differential centrifugation of cell lysates. The P13 fraction (enriched in ER membranes) and the P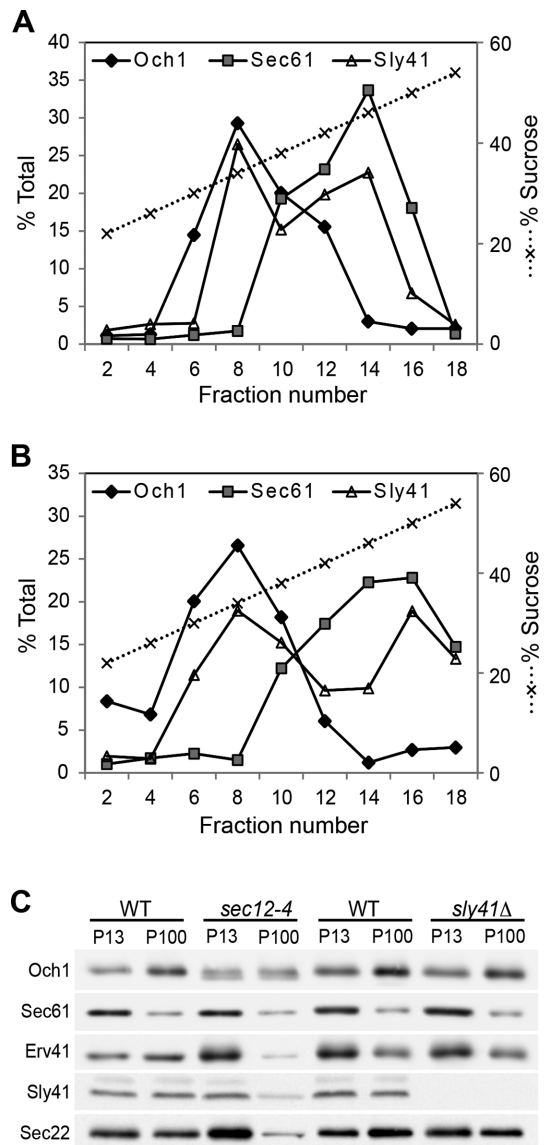100 fraction (enriched in Golgi membranes) were assessed by immunoblot (Figure 2C). The distribution of Och1 and Sec61 was not affected by the *sec12-4* block. However, Sly41 and the known cycling proteins Erv41 and Sec22 accumulated in the ER fraction of *sec12-4* cells. In addition, a *sly41Δ* strain and isogenic wild type were examined under the temperature shift, and no alterations in protein distribution were observed. Taken together, these data indicate that Sly41 cycles between the ER and Golgi compartments by means of COPII vesicles.
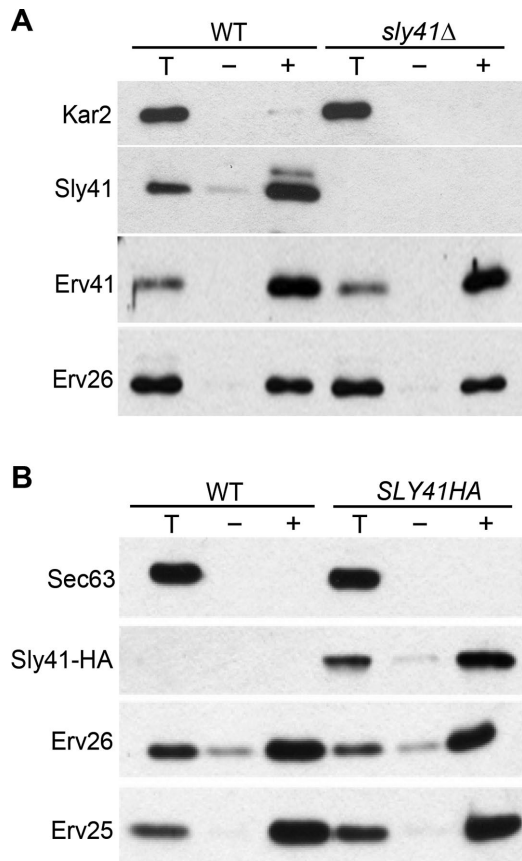
FIGURE 3: Sly41 is efficiently packaged into COPII vesicles. (A) Packaging of endogenously expressed Sly41 into COPII vesicles. Budding reactions were performed using *WT* (CBY740) and *sly41Δ* (CBY3087) microsomes. The total membranes (T) and budded vesicles in the absence (−) or presence (+) of COPII proteins were immunoblotted for Sec63 (ER marker), Erv41 and Erv26 (ER-Golgi cycling markers), and Sly41. Total lanes contain 1/10 of budding reactions. (B) Sly41-HA packaging in membranes prepared from *WT* (CBY740) and *SLY41-HA* (CBY3059) strains. One-tenth of total reactions (T) was compared with budded vesicles produced in the absence (−) or presence (+) of COPII proteins. Samples were immunoblotted with antiserums specific for Sec63 (ER resident), Erv25 and Erv26 (ER vesicle proteins), and anti-HA monoclonal antibody.

Packaging of Sly41 into COPII vesicles was assessed using a COPII budding assay. This assay was carried out by monitoring both the endogenously expressed Sly41 protein and the chromosomally HA-tagged version of Sly41. Microsomes from wild-type, *sly41Δ*, and Sly41-HA strains were incubated in the presence (+) or absence (−) of COPII proteins with an energy regeneration system to reconstitute budding (Figure 3). Membrane vesicles generated in each condition were isolated and analyzed by immunoblot as described (Belden and Barlowe, 1996). As shown in Figure 3A, Sly41 was very efficiently packaged into COPII vesicles, as were the vesicle proteins Erv41 and Erv26, whereas the ER-resident protein Kar2 served as a negative control and was not efficiently packaged in this budding assay. In *sly41Δ* budding reactions, the Sly41 immunoreactive species was absent as expected, and sorting of vesicle proteins into COPII vesicles was not influenced by this deletion. When Sly41-HA was monitored in budding reactions (Figure 3B), we again observed packaging into COPII vesicles. However, Sly41-HA was packaged less efficiently into COPII vesicles (15%)

than with untagged Sly41 protein (25%). Reduced packaging may reflect the presence of COPI and/or COPII sorting signals at the C-terminus of Sly41, which enables efficient ER/Golgi trafficking. We next investigated this idea through analysis of mutations in the C-terminus of Sly41.

Sly41 possesses C-terminal sorting motifs important for ER/Golgi trafficking

COPI mediates retrograde trafficking from the Golgi to the ER and within Golgi compartments, sorting transmembrane proteins bearing C-terminal dilysine motifs (KKXX or KXKXX). Proteins with dilysine motifs include yeast Emp47 and its mammalian orthologue, ERGIC-53, which cycle between the ER and Golgi (Schindler *et al.*, 1993; Schröder *et al.*, 1995; Teasdale and Jackson, 1996). The dilysine motif is recognized by specific COPI subunits (Cosson and Letourneur, 1994; Jackson *et al.*, 2012), and dilysine-tagged transmembrane cargo are packaged into COPI-coated vesicles for retrograde transport to the ER (Letourneur *et al.*, 1994). Sequence analysis of Sly41 revealed a C-terminal dilysine motif (SKKDGRQA); however these dilysine residues are not in the canonical -3, -4 or -3, -5 positions. Nonetheless, this motif could play an important role in the function and ER–Golgi trafficking of Sly41.

To investigate whether this motif functions in ER/Golgi trafficking, a truncation mutant of Sly41 (Sly41ΔC) lacking seven residues from the C-terminus was generated in which the first residue of the dilysine motif (K447) was mutated to a stop codon and expressed in a *sly41Δ* strain. Steady-state expression levels of Sly41 and Sly41ΔC in semi-intact cells were similar (Figure 4A), although Sly41ΔC was shifted to a lower–molecular weight range as expected. Microsomes prepared from strains overexpressing Sly41 or Sly41ΔC were analyzed in COPII budding assays to assess the role of the C-terminus in vesicle packaging (Figure 4B). Of interest, we observed that the level of Sly41ΔC in ER-enriched microsomes (total lanes) was significantly lower than with wild-type Sly41 levels. Moreover, the residual Sly41ΔC in microsomes was inefficiently packaged into COPII vesicles. These results indicate that deletion of the C-terminal residues causes mislocalization of Sly41ΔC, which is most likely due to a failure in COPI-dependent retrieval from Golgi membranes to the ER. These findings also provide evidence that COPII sorting information may be contained within the C-terminal residues of Sly41. Finally, this characterization of Sly41ΔC permits us to test the role of Sly41 trafficking in suppression of ER–Golgi tethering mutants.

Sly41 is a multicopy suppressor of tethering mutants that depends on C-terminal sorting signals and the Sec22 R-SNARE

Previous genetic studies identified Sly41 as a multicopy suppressor of loss of tethering factors Ypt1 and Uso1 (Dascher *et al.*, 1991; Ossig *et al.*, 1991; Kito *et al.*, 1996). To determine whether multicopy *SLY41* specifically suppresses tethering mutants or more generally suppresses other ER/Golgi trafficking mutants, we transformed several thermosensitive strains with multicopy *SLY41* or an empty vector control and monitored growth at 25 and 37°C. As expected, multicopy *SLY41* suppressed the temperature sensitivity of tethering mutants *ypt1-3* and *uso1-1* (Figure 5). In contrast, multicopy *SLY41* suppression was not observed in mutants deficient in COPII budding (*sec23-1*), vesicle fusion (*sly1-ts*, *sec22Δ*, *sed5-1*), or intra-Golgi transport (*cog2-1*, *ypt6Δ*, or *sec21-1*). These findings expand on previous suppression analyses (Ossig *et al.*, 1991) and suggest that *SLY41* overexpression selectively
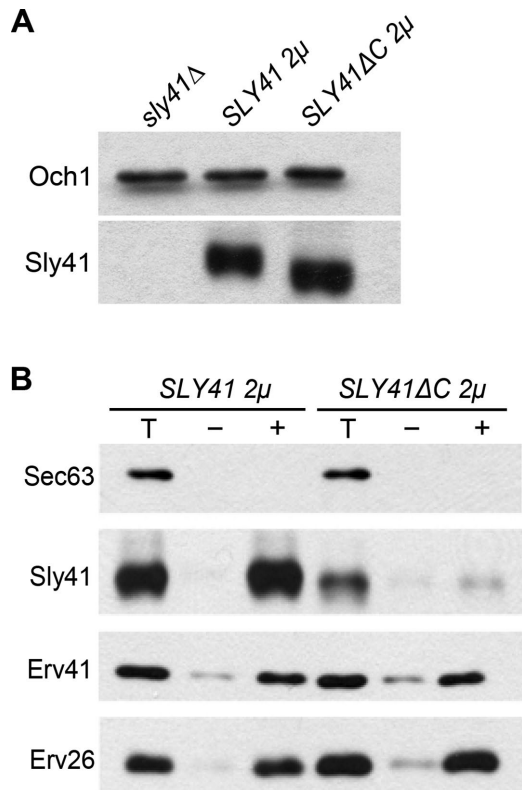
A

Och1

Sly41

B

SLY41 2μ   SLY41ΔC 2μ

T   −   +   T   −   +

Sec63

Sly41

Erv41

Erv26

FIGURE 4: Sly41ΔC is stably expressed but not efficiently packaged into COPII vesicles. (A) Semi-intact cells prepared from *sly41Δ* (CBY3087), *SLY41* 2μ (CBY3346), and *SLY41ΔC* 2μ (CBY3345) strains were immunoblotted for Och1 (loading control) and Sly41 to assess whole- cell expression levels of Sly41. (B) In vitro COPII budding reactions using microsomes prepared from *SLY41* 2μ (CBY3346) and *SLY41ΔC* 2μ (CBY3345) strains. One-tenth of total reactions (T) was compared with budded vesicles produced in the absence (−) or presence (+) of COPII proteins. Samples were immunoblotted using antisera for Sec63 (ER resident), Erv41 and Erv26 (ER vesicle proteins), and Sly41. Note that less Sly41ΔC is present in the total reaction microsomes (T) compared with Sly41.

suppresses deficiencies in the Ypt1- and Uso1-dependent tethering stage of COPII vesicles with Golgi membranes.

To further investigate the requirements for *SLY41* suppression of tethering defects, we tested whether suppression depended on the downstream ER-Golgi SNARE machinery or whether multicopy *SLY41* could bypass this step. A haploid *ypt1-3* strain lacking the Sec22 R-SNARE was constructed. In the *ypt1-3 sec22Δ* double-mutant strain, viability was maintained by expression of *SEC22* on a *URA3*-linked plasmid. Loss of the *SEC22-URA3* plasmid, indicative of Ypt1 and Sec22 bypass, was scored by growth on medium containing 5-fluoroorotic acid (5-FOA). No growth of the *ypt1-3 sec22Δ* strain with multicopy *SLY41* was observed on 5-FOA plates at 30°C (Supplemental Figure S3). This genetic test shows that a requirement for Sec22, and presumably the SNARE-mediated membrane fusion step in ER–Golgi transport, is not bypassed during suppression of tethering defects by multicopy *SLY41*.

To determine whether ER–Golgi trafficking of overexpressed Sly41 was required for suppressor activity, we compared growth of *ypt1-3* and *uso1-1* thermosensitive strains containing 2μ *SLY41* or *SLY41ΔC*. We observed that multicopy *SLY41ΔC* failed to suppress the growth defects of *ypt1-3* and *uso1-1*, in contrast to multicopy *SLY41* at restrictive temperatures (Figure 5). These results indicate
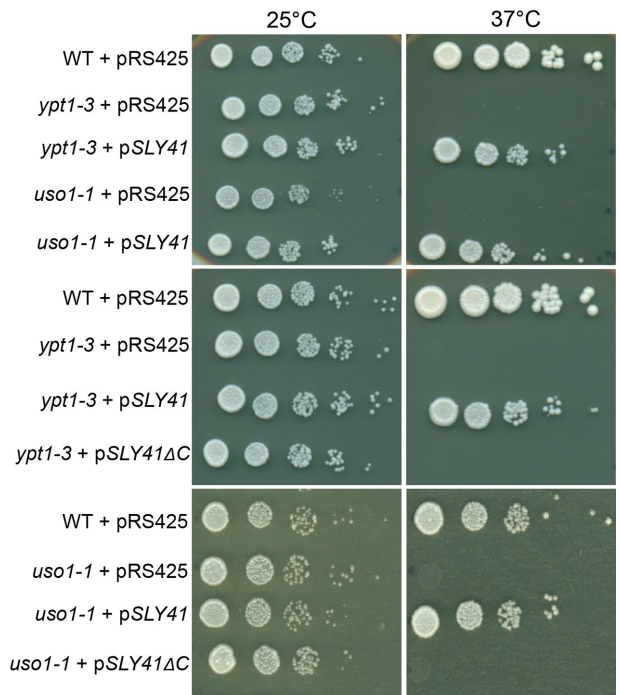
FIGURE 5: *SLY41* is a multicopy suppressor of *ypt1-3* and *uso1-1* strains. Multicopy *SLY41* suppression of *ypt1-3* (CBY830) and *uso1-1* (CBY300) compared with the wild type (CBY80) at room temperature and a restrictive temperature (37°C). Cells were precultured in CSMD minus leucine and spotted onto YPD plates. Note that *SLY41ΔC* fails to suppress the temperature sensitivity of both the *ypt1-3* (CBY830) and *uso1-1* strains (CBY300).

that C-terminal sorting signals in Sly41 are required for suppression of tethering deficiencies. Even though cells express comparable levels of Sly41 and Sly41ΔC, localization and trafficking within the early secretory pathway is critical for Sly41 suppressor activity.

Influence of Sly41 expression level on in vitro ER–Golgi transport assays

To explore the mechanism by which elevated levels of Sly41 suppress defects in vesicle tethering, we used a cell-free transport assay to test whether overexpressed Sly41 could rescue the transport defect observed in membranes prepared from *ypt1-3* mutant cells. Semi-intact cell membranes prepared from wild-type and *ypt1-3* cells bearing an empty vector or multicopy *SLY41* were used in reconstituted assays that measure COPII-dependent vesicle transport of [^{35}S]glyco-pro-α-factor (gpαf). In this assay, delivery of gpαf to Golgi membranes results in addition of outer-chain α1,6-mannose residues to the core oligosaccharide, and quantitative immunoprecipitation with α1,6-mannose–specific antibodies serves as a reporter on transport of [^{35}S]gpαf to the Golgi complex. Mutant *ypt1-3* membranes displayed transport defects in vitro compared with wild-type membranes (Figure 6A), consistent with our previous studies (Cao *et al.*, 1998). We observed that multicopy *SLY41* reversed the transport defect observed in *ypt1-3* membranes to an apparent level above that of wild-type membranes (Figure 6A). These results suggest that elevated levels of Sly41 can compensate for reduced Ypt1 activity in the in vitro transport assay. We also tested whether membranes lacking Sly41 affected ER–Golgi transport in vitro. Here the apparent level of [^{35}S]gpαf transport to the Golgi complex was not detectably altered in *sly41Δ* membranes compared with
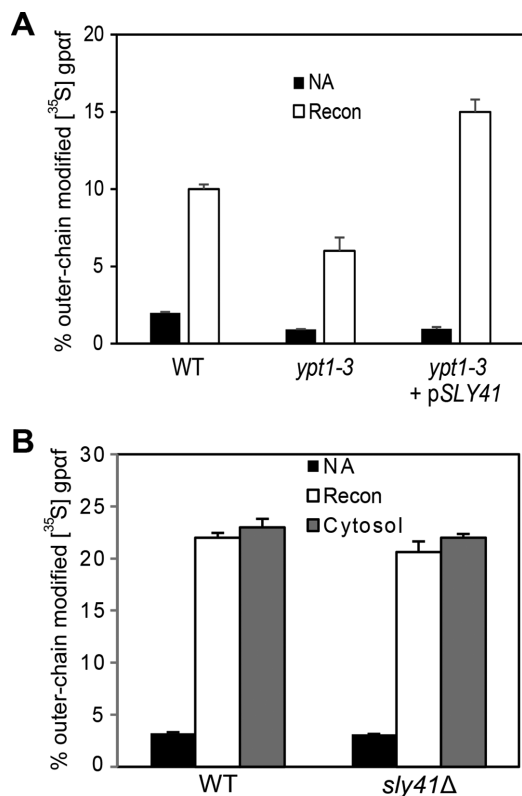
FIGURE 6: *SLY41* overexpression restores cell-free transport in the *ypt1-3* tethering mutant. (A) Transport and Golgi modification of [^{35}S] gpαf was measured in washed semi-intact cells prepared from WT (CBY80), *ypt1-3* (CBY830), and *ypt1-3* p*SLY41* 2 μ (CBY3329) strains. Reactions contained ATP regeneration system and no addition (NA) or purified transport factors (Recon: COPII, Uso1, and LMA1) and were incubated at 23°C for 60 min. The percent outer-chain modified represents the amount of total [^{35}S]gpαf that had been modified by the addition of Golgi-specific α1,6-mannose residues. (B) *sly41Δ* does not display transport defects in vitro. Transport and Golgi modification of [^{35}S]gpαf was measured in washed semi-intact cells prepared from WT (CBY740) and *sly41Δ* (CBY3087) strains. Reactions contained no addition (NA), purified transport factors (Recon: COPII, Uso1, and LMA1), or crude cytosol and were incubated at 23°C for 60 min. Golgi-modified [^{35}S]gp-α-factor was measured as described.

FIGURE 7: *SLY41* overexpression increases transport and Golgi modification of [^{35}S]gpαf in vitro. (A) Golgi-modified [^{35}S]gpαf was measured in WT (CBY80) and WT + p*SLY41* 2μ (CBY3346) semi-intact cells. Reactions contained ATP regeneration system and no addition (NA) or purified transport factors (Recon: COPII, Uso1, and LMA1) and were incubated at 23°C for 60 min. The percentage of outer-chain modified [^{35}S]gpαf represents the fraction that contains Golgi-specific α1,6-mannose residues. (B) COPII budding and vesicle tethering in WT (CBY80) and WT + p*SLY41* 2μ (CBY3346) semi-intact cells. Washed semi-intact cells were incubated with no addition (NA), COPII proteins (COPII), or COPII and Uso1 (COPII + Uso1) at 23°C for 30 min. The percentage of [^{35}S]gpαf in diffusible vesicles represents protease-protected [^{35}S]gpαf released into the medium-speed supernatant fraction divided by total protected [^{35}S]gpαf. Note that *SLY41* overexpression does not influence levels of COPII budding or Uso1-dependent vesicle tethering.

wild-type membranes when transport was supported by purified transport factors or crude cytosol (Figure 6B).

To further investigate the influence of Sly41 overexpression in cell-free transport assays, we directly compared wild-type membranes with membranes that contained overexpressed levels of Sly41. Surprisingly, Sly41-overexpressing membranes displayed a 1.5-fold increase in outer-chain modified [^{35}S]gpαf as compared with wild-type membranes transformed with an empty vector (Figure 7A). Because multicopy *SLY41* suppresses tethering defects in vivo, we also carried out in vitro tethering assays using the wild-type and Sly41 overexpressor strains. We did not observe significant differences in the efficiency of vesicle budding or Uso1-dependent tethering of vesicles between the two strains (Figure 7B). To further characterize the increase in Golgi-modified [^{35}S]gpαf observed in the Sly41 overexpressor membranes, we conducted a kinetic analysis of cell-free transport (Supplemental Figure S4). In accord with the endpoint assays, Sly41 overexpression produced an increased rate of outer-chain modified [^{35}S]gpαf as compared with the wild type over this entire time course. Because COPII vesicle budding and
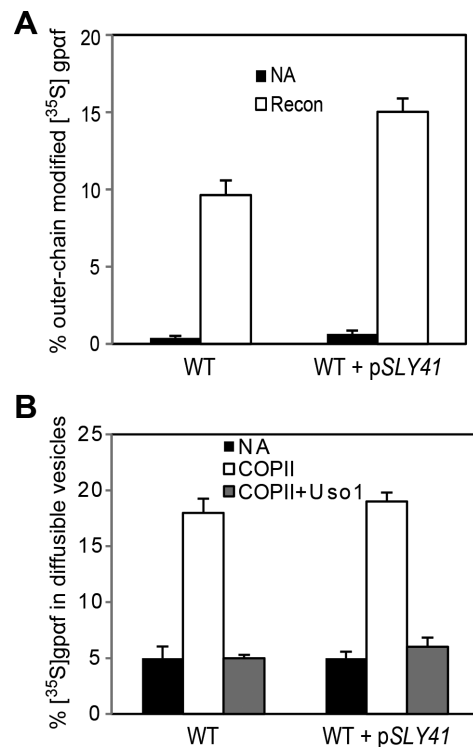
tethering were not altered by Sly41 expression, these results suggest that Sly41 overexpression increases the rate of the SNARE-dependent vesicle fusion stage and/or the subsequent outer-chain modification reaction of [^{35}S]gpαf.

On the basis of these collective results, we tested for Sly41 associations with proteins involved in COPII vesicle tethering and fusion. However, we detected no specific interactions between Sly41 and known components of the ER–Golgi fusion machinery through native and cross-linking immunoprecipitation approaches. Although these results do not rule out direct interactions, we next investigated the hypothesis that membrane transporter activity of Sly41 could explain our genetic and in vitro findings. As a member of the SLC family, overexpression of Sly41 may alter membrane properties or change solute concentrations in cytosol and luminal compartments.

SLY41 interacts genetically with *PMR1* and affects cytosolic levels of Ca²⁺

The SLC family of transporters is divided into subfamilies based on criteria that include sequence homology, structural features, and substrates transported. Several members of the SLC family have

been extensively characterized and are known to transport diverse substrates, including amino acids, sugars, nucleotides, and vitamins, as well as inorganic cations and anions (Hediger *et al.*, 2004; Hoglund *et al.*, 2011). Sly41 belongs to the SLC35 family of proteins based on sequence homology, and while some members of this family are known nucleotide sugar transporters, the Sly41 subgroup (SLC35E) comprises orphan transporters with no known physiological substrates (Hadley *et al.*, 2014). Other characterized nucleotide sugar transporters operate as antiporters, by which import of a nucleotide sugar is typically exchanged with its corresponding nucleotide monophosphate (Caffaro and Hirschberg, 2006). Therefore overexpressed Sly41 could exert suppressive effects by transporting substrates into the luminal compartment or counter ions out of the lumen.

We examined the literature for genetic interactions between *SLY41* and other genes that encode transporters, as well as for examples in which transporter activity influenced trafficking in the early secretory pathway. The Ca^{2+} transporter Pmr1 and Ca^{2+} levels were reported to influence ER–Golgi trafficking. Pmr1 is a Golgi-localized Ca^{2+}/Mn^{2+} ATPase that mediates high-affinity transport of Ca^{2+} and Mn^{2+} into the luminal compartments of the early secretory pathway, which is needed for a variety of secretory functions, including protein folding, processing, and glycosylation (Rudolph *et al.*, 1989; Durr *et al.*, 1998; Mandal *et al.*, 2000). Of interest, addition of calcium to growth medium was also reported to relieve growth defects in *YPT1* and *USO1* mutants, although the mechanism of this suppression is unknown (Schmitt *et al.*, 1988; Kito *et al.*, 1996). These studies prompted us to test whether *SLY41* overexpression or deletion would influence *pmr1Δ* mutant phenotypes.

It is known that *pmr1Δ* deletion mutants are hypersensitive to chelating agents (ethylene glycol tetraacetic acid [EGTA], 1,2-bis(o-aminophenoxy)ethane-N,N,N′,N′-tetraacetic acid [BAPTA]) when added to the growth medium (Rudolph *et al.*, 1989; Durr *et al.*, 1998). Of interest, we observed that *sly41Δ pmr1Δ* double mutants were more sensitive to chelating agents in growth medium than were the single-deletion parent strains (Figure 8A). This indicates that *sly41Δ* and *pmr1Δ* display negative genetic interactions when divalent cation concentrations are limiting. Surprisingly, overexpression of *SLY41* in a *pmr1Δ* background did not yield any significant changes in sensitivity to chelating agents (Figure 8B). This result suggests that *SLY41* and *PMR1* do not simply provide redundant activities. However, the novel synthetic negative interaction between *sly41Δ* and *pmr1Δ* is interesting because *pmr1Δ* was reported to suppress the cold-sensitivity phenotype of a *ypt1-1* strain (Rudolph *et al.*, 1989; Antebi and Fink, 1992). On the basis of these observations, we hypothesized that Sly41 overexpression could influence cytosolic levels of divalent cations such as Ca^{2+}.

To test this hypothesis, we used an aequorin-based assay to monitor and compare changes in cytosolic Ca^{2+} levels in different strains. We analyzed wild-type, *sly41Δ*, *pmr1Δ*, and *SLY41* overexpressor strains and calculated levels of $[Ca^{2+}]_{cyt}$. Basal levels of 0.25 μM $[Ca^{2+}]_{cyt}$ were observed in wild-type and *sly41Δ* strains, which are similar to previously reported levels (Demaegd *et al.*, 2013). As expected, the *pmr1Δ* strain displayed greater $[Ca^{2+}]_{cyt}$ levels of ~0.5 μM as compared with wild type. Strikingly, the *SLY41* overexpressor strain also displayed elevated $[Ca^{2+}]_{cyt}$ levels of ~0.4 μM, which is significantly greater than observed in wild-type cells (Figure 9A). Although the absence of Sly41 did not yield detectable changes in $[Ca^{2+}]_{cyt}$ levels, this could be due to limitations of the aequorin-based assay or the possibility that the growth conditions used in our experiments could dampen minor changes. Nonetheless, these results clearly indicate that Sly41 expression level
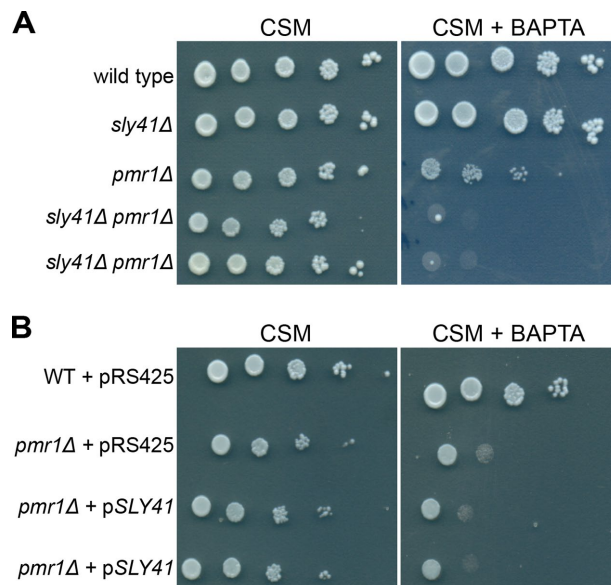
FIGURE 8: *SLY41* displays a negative genetic interaction with *PMR1*. (A) *WT* (CBY740), *sly41Δ* (CBY3087), *pmr1Δ* (CBY1573), and two independent isolates of *sly41Δ pmr1Δ* (CBY3562, CBY3563) were tested on CSM plates with and without 1.6 mM BAPTA at 30°C. (B) *WT* (CBY740) and *pmr1Δ* (CBY1573) strains expressing empty vector and *pmr1Δ* expressing p*SLY41* were tested on CSM plates with and without 1.6 mM BAPTA at 30°C. Two independent transformants of *pmr1Δ* p*SLY41* (CBY4320, CBY4321) were grown to saturation in appropriate medium to maintain plasmid selection and spotted onto plates.

influences cytosolic Ca^{2+} concentrations in the cell. Moreover, elevated cytosolic Ca^{2+} levels resulting from Sly41 overexpression can explain the suppression of specific COPII vesicle–tethering mutants analogous to *pmr1Δ* suppression of *ypt1-1* (Antebi and Fink, 1992).

The observed increase in basal cytosolic Ca^{2+} levels could be due to whole-cell increases in Ca^{2+} levels upon Sly41 overexpression or to a redistribution of the calcium stores within the cell. To examine these possibilities, we carried out whole-cell analysis using inductively coupled plasma mass spectrometry (ICP-MS) of wild-type, *sly41Δ*, *pmr1Δ*, and *SLY41* overexpressor strains. As reported previously, the *pmr1Δ* strain displayed higher whole-cell levels of calcium (Halachmi and Eilam, 1996). Similarly, the Sly41 overexpressor also displayed an increase in whole-cell levels of Ca^{2+} compared with the wild type (Figure 9B). These results further support a role for Sly41 in cellular calcium homeostasis.

To determine whether elevated Ca^{2+} levels and *SLY41* overexpression suppress tethering deficiencies through a similar mechanism, we again tested whether calcium suppression of *ypt1-3* temperature sensitivity depended on the Sec22 R-SNARE. As shown in Supplemental Figure S3, addition of calcium to the growth medium can effectively suppress the temperature sensitivity of a *ypt1-3* strain; however, this condition does not suppress growth defects of a *ypt1-3 sec22Δ* double-mutant strain. These genetic analyses indicate that calcium-mediated suppression of *ypt1-3* does not bypass a requirement for the ER–Golgi SNARE fusion machinery, as observed for *SLY41*-mediated suppression of this tethering deficiency (Supplemental Figure S3).

Mn^{2+} and Ca^{2+} influence cell-free transport assays

Our data indicate that Sly41 overexpression elevates intracellular calcium levels, as observed for *pmr1Δ* mutants in suppressing
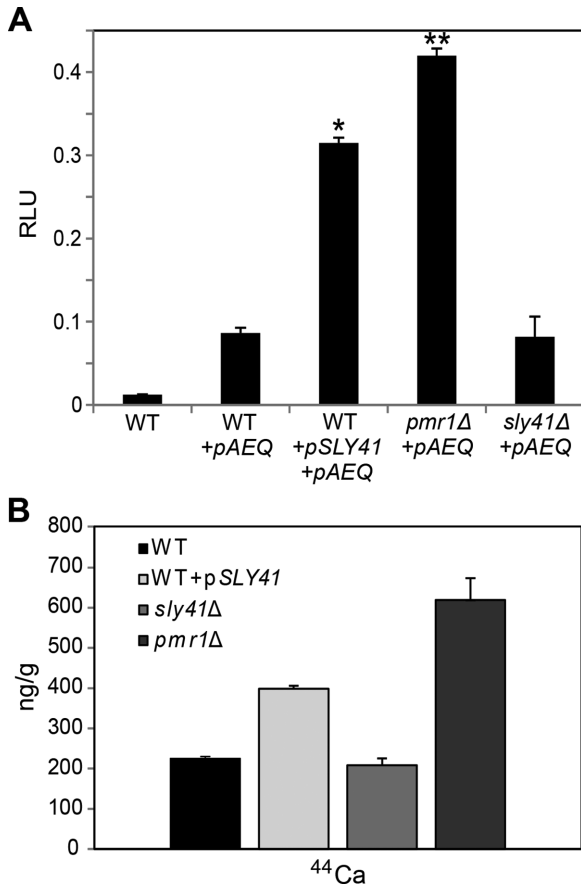
FIGURE 9: *SLY41* overexpression increases intracellular levels of calcium. (A) Determination of basal cytosolic Ca^{2+} levels using coelenterazine-treated, apoaequorin-expressing cells. Endpoint measurements were carried out for 20 s. Wild type without the apoaequorin plasmid and apoaequorin-expressing *WT* (CBY3745), *sly41Δ* (CBY3746), *pmr1Δ* (CBY3753), and p*SLY41* 2μ (CBY3743) strains were compared. All displayed results are representative of those seen with at least three replicates. **$p < 0.01$ and *$p < 0.05$ (B) Determination of whole-cell levels of Ca^{2+} using ICP-MS. *WT* (CBY2069), p*SLY41* 2μ (CBY3334), *sly41Δ* (CBY3341), and *pmr1Δ* (CBY3755) strains were grown to log phase, harvested, and digested with nitric acid at 75°C for 40 min. The samples were then analyzed using the Agilent ICP-MS system.

Ypt1-dependent tethering. However, it is also known that Pmr1 is a high-affinity transporter for both Ca^{2+} and Mn^{2+} into luminal compartments of the early secretory pathway. Therefore we examined the effect of these divalent cation levels on cell-free vesicle fusion assays. This analysis is complicated because the standard readout for vesicle fusion is Golgi-specific outer-chain modification of [^{35}S]gpαf, which depends on both of these divalent cations (Baker *et al.*, 1990; Flanagan and Barlowe, 2006). More specifically, the mannosyltransferase enzymes that add outer-chain α1,6-mannose residues require Mn^{2+} for activity (Romero and Herscovics, 1989), and transport of GDP-mannose into Golgi compartments relies on the Ca^{2+} dependent GDPase activity to generate luminal GMP needed in exchange (Yanagisawa *et al.*, 1990; Berninsone *et al.*, 1994). Previous studies showed that addition of divalent cation chelators such as EGTA strongly decreased apparent transport through inhibition of the outer-chain modification reaction but does not block SNARE-dependent membrane fusion (Flanagan and Barlowe, 2006; Flanagan *et al.*, 2015). These find-

ings show that divalent cations are not directly required for fusion of COPII vesicles with Golgi membranes, although Mn^{2+} or Ca^{2+} could still perform regulatory roles in this membrane fusion stage.

To monitor the effect of Mn^{2+} on cell free transport assays, we conducted reactions in which semi-intact cells containing translocated [^{35}S]gpαf were incubated with purified transport factors in the presence or absence of added $MnCl_2$. Surprisingly, titration experiments revealed that addition of 1 mM $MnCl_2$ increased levels of outer-chain modified [^{35}S]gpαf approximately twofold (Figure 10A). Stimulation by added $MnCl_2$ indicates that the standard cell-free transport conditions with washed membranes are limiting for Mn^{2+}. This effect is probably due to suboptimal levels of luminal Mn^{2+} needed for outer-chain modification of [^{35}S]gpαf by Golgi mannosyltransferases (Romero and Herscovics, 1989). Of interest, the *sly41Δ* acceptor membranes displayed greater stimulation of outer-chain modified [^{35}S]gpαf at intermediate concentrations of $MnCl_2$ compared with wild-type acceptor membranes (Figure 10A). This effect was also observed over a time course of the cell-free assay at 0.5 mM $MnCl_2$ (Supplemental Figure S5), indicating that addition of $MnCl_2$ influenced the rate of outer-chain modification and not overall integrity of membranes in the reaction. In contrast, transport reactions with acceptor membranes prepared from the Sly41 overexpressor strain displayed increased [^{35}S]gpαf modification, as observed earlier in Figure 7A; however, stimulation by added $MnCl_2$ was less than observed for wild-type membranes (unpublished data). These findings suggest that *sly41Δ* Golgi membranes may contain reduced levels of Mn^{2+}, whereas overexpression of Sly41 increases Mn^{2+} levels in the Golgi lumen to stimulate levels of outer-chain modification.

Two-stage fusion reactions were also performed over a range of Ca^{2+} concentrations to test the influence of Ca^{2+} on this cell-free assay. Reconstituted fusion reactions were conducted in which isolated COPII vesicles containing [^{35}S]gpαf were incubated with washed semi-intact cells that contain Golgi acceptor membranes. Addition of $CaCl_2$ produced modest effects on the level of outer-chain modified [^{35}S]gpαf, with increased levels observed at 0.5 μM $CaCl_2$, whereas concentrations of ≥10 μM decreased this signal (Figure 10B). In the presence of 0.1 mM $MnCl_2$, similar results were observed with stimulation at 0.5 μM $CaCl_2$, and overall levels of modified [^{35}S]gpαf increased by addition of Mn^{2+} to reactions (Figure 10C). In analyses of *sly41Δ* and Sly41 overexpressor membranes, we were not able to detect clear differences compared with wild-type membranes when Ca^{2+} concentrations were varied. These results suggest that Mn^{2+} and Ca^{2+} influence the cell-free fusion assay by distinct mechanisms. Because the readout of this in vitro assay depends on rates of SNARE-dependent membrane fusion in addition to rates of outer-chain α1,6-mannose addition, it is difficult to distinguish the stages in which these divalent cations act. Therefore we next used a SNARE cross-linking assay to monitor directly the membrane fusion stage of COPII vesicles with Golgi membranes.

Ca^{2+} increases membrane fusion rates measured by a SNARE cross-linking assay

To determine whether physiological concentrations of Ca^{2+} influence rates of COPII vesicle fusion with Golgi membranes, we used an in vitro assay that measures assembly of new SNARE complexes produced when these membranes fuse. In previous work, we introduced unique cysteine residues into ER–Golgi SNARE proteins such that when donor and acceptor membranes fuse, adjacent cysteine residues in newly assembled SNARE complexes form disulfide cross-links under oxidizing conditions (Flanagan and Barlowe, 2006).
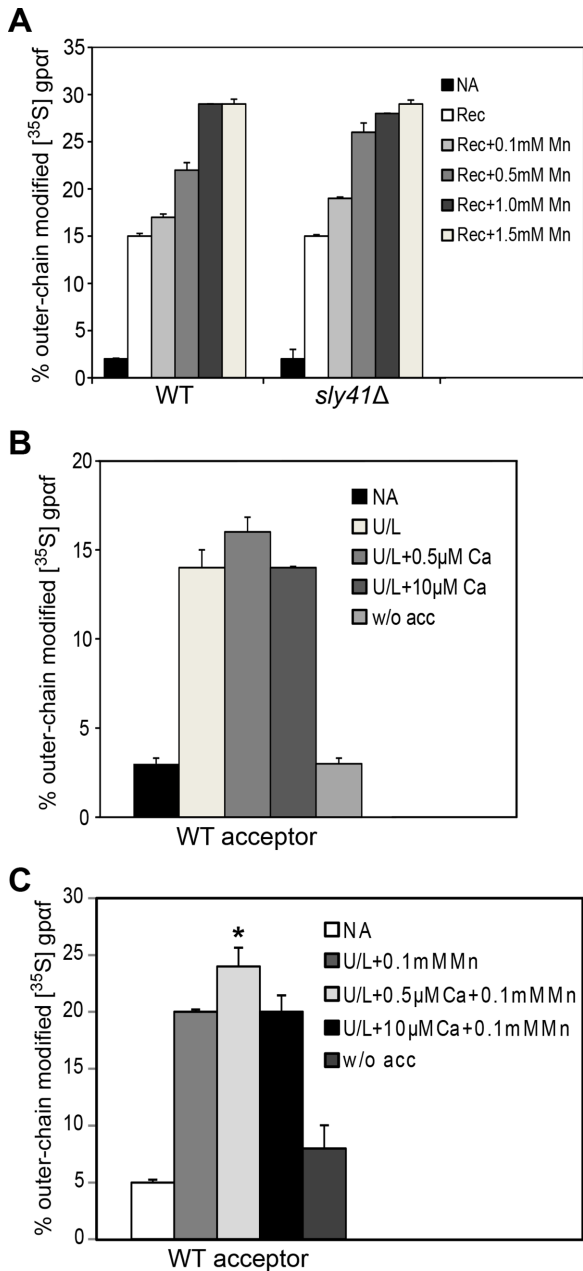
FIGURE 10: Mn²⁺ increases the extent of outer-chain [³⁵S]gpαf modification. (A) Outer-chain modification measured in *WT* (CBY740) and *sly41Δ* (CBY3087) semi-intact cells with ATP regeneration system and no addition (NA) or with reconstituted transport factors COPII, Uso1, and LMA1 (Rec). MnCl₂ was added from 0.1 to 1.5 mM where indicated, and reactions were incubated at 23°C for 60 min. The percentage of outer-chain modified [³⁵S]gpαf represents the fraction of [³⁵S]gpαf that contains Golgi-specific α1,6-mannose residues. (B) Two-stage transport reactions in which COPII vesicles were isolated and incubated with washed semi-intact cell acceptor membranes (CBY740 WT strain) at 23°C for 60 min. Uso1/LMA1 (U/L) and CaCl₂ were added as indicated. Outer-chain modified [³⁵S]gpαf was measured as described. (C) Two-stage transport reactions as in B. Uso1/LMA1 (U/L), MnCl₂, and CaCl₂ were added as indicated. Modest stimulation (*$p < 0.05$) in the presence of 0.5 μm CaCl₂ was detected.

Placement of cysteine residues within the SNARE motif, transmembrane domain, or luminal segment can provide readouts for *trans*- and *cis*-SNARE complexes when analyzed on nonreducing poly-

acrylamide gels. We also observed that the R-SNARE protein Sec22 efficiently forms a homodimer that can be detected through this cross-linking approach (Flanagan *et al.*, 2015). For the present study, we set up the cysteine cross-linking assay using COPII vesicles that contain Sec22 modified with a cysteine residue at position L213 in the luminal domain. Golgi acceptor membranes were prepared from semi-intact cells expressing Sec22(L213C)-3HA. Fusion rates can then be assessed by monitoring the formation of the mixed Sec22-Sec22HA cross-linked dimer produced when COPII vesicles containing Sec22(L213C) fuse with Golgi membranes containing Sec22(L213C)-3HA.

In two-stage fusion reactions using Sec22(L213C) vesicles and washed Sec22(L213C)-3HA acceptor membranes, we observed increased formation of the Sec22-Sec22HA cross-linked product when purified fusion factors (Uso1 and LMA1) were added to the reactions (Figure 11A). This was expected and reproduces our previous results using the cross-linking assay to monitor vesicle fusion (Flanagan *et al.*, 2015). We did not detect an increase in cross-linked product using Sly41 overexpressor membranes, although these washed membranes would not preserve cytosolic levels of calcium. In addition, we were not able to recover fusion activity using mutant membranes in the SNARE cross-linking assay. However, using wild-type membranes in the absence of purified Uso1, we observed that addition of CaCl₂ produced a significant increase in the Sec22-Sec22HA cross-linked species (Figure 11A). This result suggests that Ca²⁺ can stimulate vesicle fusion when there are limiting amounts of Uso1 tethering factor. Moreover, a stepwise increase in fusion was observed from 0.3 to 0.5 μM CaCl₂, which reflects the in vivo suppression range of cytosolic Ca²⁺ levels detected using the aequorin-based assay. Note that the level of vesicle fusion in the presence of 0.5 μM CaCl₂ without added Uso1 was less than the fully reconstituted reaction. We also observed that addition of 0.5 μM CaCl₂ in combination with saturating Uso1 did not produce a detectable increase in fusion signal above the reconstituted reaction (Supplemental Figure S6). Finally, stimulation of the fusion signal by adding Ca²⁺ appears to be specific, because addition of 0.5 mM MnCl₂ did not increase levels of the Sec22-Sec22HA cross-linked product (Supplemental Figure S7). These results suggest that Uso1-dependent fusion produces a maximal signal of cross-linked SNARE product, but importantly, when Uso1 tethering activity is deficient, the addition of Ca²⁺ stimulates SNARE-dependent fusion.

We carried out a kinetic analysis of mixed Sec22(L213C)-Sec22(L213C)HA homodimer formation in reconstituted two-stage fusion reactions to compare rates in the presence of added Uso1 or in the absence of added Uso1 with 0.5 μM CaCl₂. As shown in Figure 12, a time-dependent increase in fusion signal was observed under both conditions. The kinetics of cross-linked homodimer formation was markedly increased in the presence of fusion factors compared with background levels, as previously observed (Flanagan *et al.*, 2015). The addition of 0.5 μM Ca²⁺ produced a similar gradual increase in formation of the cross-linked homodimer, although the overall rate was slower under the Ca²⁺ condition than with reconstituted reactions with added Uso1. This kinetic analysis is consistent with the endpoint assay results in Figure 11. Moreover, the gradual time-dependent progression in fusion signal observed in the presence of Ca²⁺ suggests that membrane fusion proceeds through a similar SNARE protein–dependent mechanism. We tested whether the addition of Ca²⁺ to standard COPII vesicle–tethering assays could increase tethering in the absence of added Uso1 (Figure 11B). However, no detectable increase in vesicle tethering was observed in the presence of 0.5 μM CaCl₂, suggesting that Ca²⁺ acts to stimulate the SNARE protein–dependent fusion step instead of vesicle

A

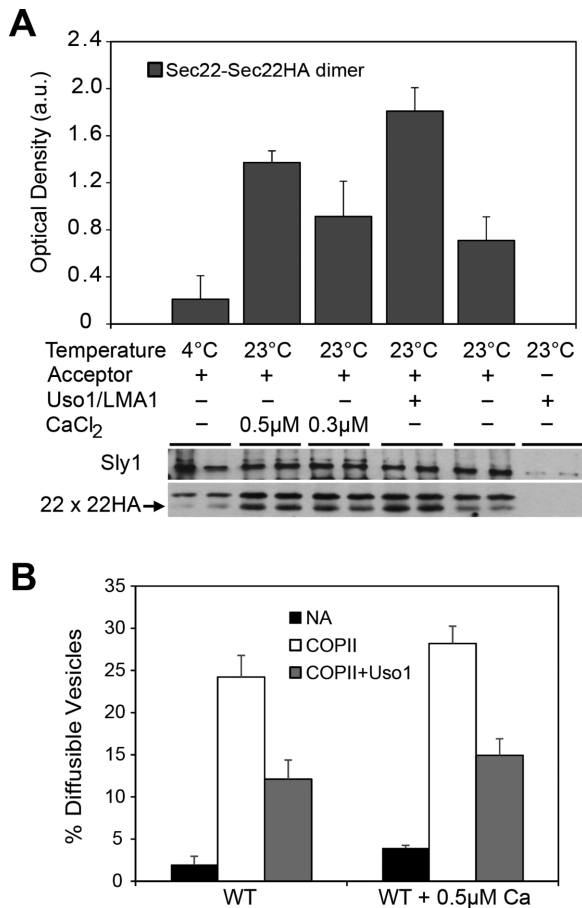| Temperature	4°C	23°C	23°C	23°C	23°C	23°C
Acceptor	+	+	+	+	+	−
Uso1/LMA1	−	−	−	+	−	+
CaCl₂	−	0.5μM	0.3μM	−	−	−

Sly1
22 × 22HA→

B

FIGURE 11: Determination of the effect of Ca²⁺ on vesicle fusion using a cysteine disulfide cross-linking assay. Two-stage transport reactions using COPII vesicles containing Sec22(L213C) and acceptor membranes with Sec22(L213C)-HA acceptor membranes were incubated in the presence of an ATP regeneration system and CaCl₂ or Uso1/LMA1 as indicated. After 60 min, the reactions were processed and proteins resolved on nonreducing polyacrylamide gels to detect the mixed Sec22-Sec22HA (22 × 22HA) cross-linked dimer by immunoblotting with anti-HA monoclonal antibodies. The Sly1 immunoblot serves as loading control. Relative levels of the 22 × 22HA dimer (gray bars) were quantified using the UN-SCAN-IT software package. (B) Addition of calcium does not affect vesicle tethering in vitro. Vesicle budding and tethering in *WT* (CBY740) semi-intact cells was assayed with COPII and Uso1 proteins in the presence or absence of 0.5μM Ca²⁺ at 23°C for 30min. The percentage of diffusible vesicles represents the amount of [³⁵S]gpαf released into a medium-speed supernatant fraction divided by the total amount of [³⁵S]gpαf contained in the reaction.

tethering. These collective findings are consistent with a model in which elevated Ca²⁺ levels can boost vesicle fusion efficiency when there is a deficiency in vesicle tethering.

DISCUSSION

In the present study, we investigate the multipass membrane protein Sly41 and characterize its influence on ER–Golgi trafficking. Sly41 was detected on COPII vesicles, and our results document efficient packaging of Sly41 into ER-derived vesicles, as well as active cycling between the ER and Golgi compartments. Cells lacking Sly41 do not display obvious growth or secretion defects, and Sly41 does not appear to act directly on the ER–Golgi fusion machinery. However, we observed synthetic negative genetic interactions between *sly41Δ*

and *pmr1Δ*, indicating that Sly41 influences cellular Ca²⁺ and/or Mn²⁺ homeostasis. Overexpression of *SLY41* caused a striking increase in cytosolic calcium levels and selectively suppressed the temperature-sensitive tethering mutants *ypt1-3* and *uso1-1*. In vitro assays to measure fusion of COPII vesicles with Golgi membranes demonstrated a corresponding increase in the SNARE protein–dependent fusion step when Ca²⁺ concentrations were elevated to suppressive cellular levels in the background of reduced tethering activity. These findings are significant because they explain longstanding questions regarding how overexpression of the Sly41 membrane transporter protein and elevated cytosolic calcium levels can suppress deficiencies in the vesicle-tethering stage of fusing ER-derived vesicles with Golgi membranes (Schmitt *et al.*, 1988; Dascher *et al.*, 1991; Kito *et al.*, 1996). Our results support a model in which Sly41 overexpression increases intracellular calcium levels, and elevated calcium then positively regulates trafficking through the early secretory pathway, specifically at the SNARE-dependent vesicle fusion stage.

How does Sly41 overexpression increase cytosolic Ca²⁺ concentrations? As a member of the SLC35 family of transporter proteins, Sly41 is a probable transporter for nucleotide sugars from the cytoplasm into the Golgi lumen, although we do not know the exact substrate(s) of the Sly41 transporter (Hadley *et al.*, 2014). In addition to our in vivo studies showing increased cytosolic Ca²⁺ when Sly41 was overexpressed, in vitro assays that follow Golgi-specific outer-chain modification of gpαf suggest that luminal concentrations of Mn²⁺ are also influenced by Sly41 expression. The mannosyltransferase enzymes responsible for adding outer-chain α1,6-mannose residues are abundant in yeast cells for cell wall biosynthesis (Orlean, 2012), and these enzymes require Mn²⁺ for activity (Romero and Herscovics, 1989; Durr *et al.*, 1998). We observed that in *sly41Δ* membranes, Mn²⁺ levels were apparently deficient, as increased outer-chain modification was detected when Mn²⁺ was added to fusion/modification reactions. Combining *sly41Δ* with *pmr1Δ* could further reduce luminal Mn²⁺ concentrations and explain their synthetic negative interaction. In contrast, outer-chain modification in Sly41 overexpressor membranes was increased and less responsive to MnCl₂ than with wild-type membranes. These observations are consistent with a model in which Sly41 activity increases Mn²⁺ levels in Golgi membranes. We speculate that in Sly41-overexpression conditions, increased nucleotide sugar transport by Sly 41 into the Golgi lumen indirectly influences Mn²⁺ transport, possibly through accumulation of nucleotide sugars or increased production of nucleotides and phosphate that are generated by the luminal glycosylation machinery (Berninsone *et al.*, 1994; Gao *et al.*, 1999; Orlean, 2012). These altered luminal concentrations could inhibit Mn²⁺ efflux from Golgi compartments by the Atx2 transporter (Lin and Culotta, 1996) or stimulate uptake by Smf1/Smf2 transporters (Portnoy *et al.*, 2000; Garcia-Rodriguez *et al.*, 2015). Alternatively, Sly41 could directly transport Mn²⁺ into the Golgi lumen through some type of low-affinity symport mechanism, as reported for the Pho84 phosphate transporter (Jensen *et al.*, 2003). Ultimately, the net effect of Sly41 overexpression is elevated Ca²⁺ concentrations in cytosol and in whole cells, an effect similar to that in *pmr1Δ* mutants. On the basis of these results, we propose that Sly41 overexpression first increases luminal levels of Mn²⁺, which results in inhibition of Ca²⁺ uptake by Golgi transporters and elevation of cytosolic calcium. This could also explain why multicopy *SLY41* does not suppress the *pmr1Δ* mutant, because luminal Ca²⁺ levels would remain low.

It is important to note that proper localization of Sly41 to ER and Golgi membranes is required for its suppressive activity, as revealed by the trafficking-defective Sly41ΔC mutant. This result indicates that localized overlap of Sly41 with the Golgi glycosylation
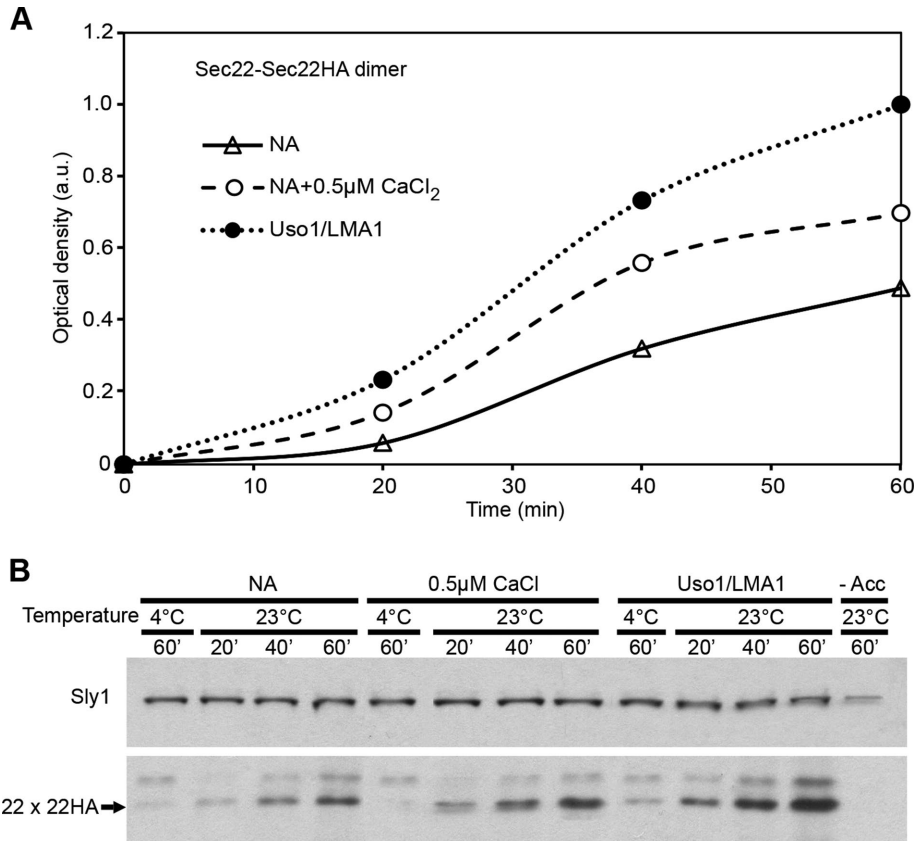
A

B

FIGURE 12: Time course of the effect of Ca²⁺ on vesicle fusion using the disulfide cross-linking assay. (A) Two-stage transport reactions using COPII vesicles containing Sec22(L213C) and Sec22(L213C)-HA acceptor membranes were incubated in the presence of an ATP regeneration system alone (NA) and with CaCl₂ or Uso1/LMA1 as indicated. (B) The reactions were incubated at 23°C for 20, 40, and 60 min and then processed to determine the levels of Sec22-Sec22HA cross-linked dimer formed. Sly1 immunoblot serves as a loading control and used to normalize the levels of Sec22-Sec22HA cross-linked product, which were quantified using the UN-SCAN-IT software package.

be the calcium-binding calmodulin protein (Colombo *et al.*, 1997; Peters and Mayer, 1998; Cao *et al.*, 2015), and Rab GAP proteins (Parkinson *et al.*, 2014). Several studies indicate that Ca²⁺ levels influence trafficking through the early secretory pathway (Hay, 2007), although specific molecular targets that act in membrane fusion steps are not well established. Recent studies show that ER budding involves the calcium-binding ALG-2 protein, which interacts with COPII to retain the coat on vesicles and decrease fusion rate (Helm *et al.*, 2014). However, calmodulin or synaptotagmin-like proteins are not known to operate in SNARE-dependent fusion steps in trafficking between the ER and Golgi.

Our experiments monitoring the formation of cross-linked Sec22 homodimers as a direct reporter on fusion of COPII vesicles with Golgi membranes showed that addition of calcium in the absence of maximal tethering stimulated membrane fusion. When Uso1 was present at saturating levels, Ca²⁺ addition did not detectably increase formation of the cross-linked SNARE product. Moreover, the addition of Ca²⁺ could not promote COPII vesicle tethering to Golgi membranes in the absence of Uso1. These findings indicate that Ca²⁺ does not substitute for Uso1-dependent tethering but instead bypasses the need for efficient vesicle tethering. These results are also consistent with our previous studies showing that in the presence of maximal fusion factors, EGTA addition does not inhibit formation of cross-linked fusion dimers but inhibits the outer-chain modification of gpαf that occurs postfusion (Flanagan and Barlowe, 2006; Flanagan *et al.*, 2015). We conclude that Ca²⁺ is not required but stimulates the SNARE-dependent fusion stage in the absence of optimal vesicle tethering. We hypothesize that Ca²⁺ could act directly on the ER–Golgi SNARE proteins or Sly1 to promote assembly and catalyze membrane fusion. It is also possible that uncharacterized calcium-binding protein(s) present on COPII vesicles or Golgi membranes could assist in this process. Alternatively, Ca²⁺ is known to bind and influence the biophysical properties of phospholipid bilayers (Feigenson, 1986; Mao *et al.*, 2013). Indeed, Ca²⁺ interactions with acidic phospholipids are reported to increase rates of lipid mixing and promote fusion pore formation in model membrane fusion systems (Tarafdar *et al.*, 2012). In these studies, calcium binding is proposed to reduce the energy barrier of membrane clustering to produce hemifused intermediates and then stabilize highly curved membrane structures that arise during fusion pore formation. Calcium is also reported to promote negative or positive membrane curvature, depending on lipid composition and ionic concentrations (Yaghmur *et al.*, 2011; Simunovic *et al.*, 2015). Membrane curvature is known to influence fusogenicity of many biological membranes (Martens and McMahon, 2008). Although the effects of Ca²⁺ on certain membrane compositions may be generalizable, we note that elevated calcium levels are not reported to suppress deficiencies in other Rab GTPase/tethering-dependent stages of the yeast secretory pathway. These

machinery and Golgi transporters such as Pmr1 is needed for elevated Ca²⁺ levels and suppression of tethering mutants. These findings also support the view that the Golgi apparatus serves as an important intracellular calcium store and functions in maintaining cellular calcium homeostasis (Micaroni, 2012).

Calcium has been implicated in membrane fusion at multiple intracellular trafficking events (Hay, 2007). Perhaps the best-understood mechanism is based on studies of synaptic vesicle exocytosis, in which an action potential stimulates Ca²⁺ influx through channels positioned at the active zone. Transiently elevated Ca²⁺ then binds to a clamp consisting of the calcium-binding synaptotagmin protein and complexin, which holds partially zippered SNARE complexes in a fusion-ready state. When Ca²⁺ binds synaptotagmin, conformational changes alter the clamp in a way that completes SNARE complex assembly and displaces complexin to trigger vesicle fusion (Sudhof, 2013). Neurotransmitter release through fusion of synaptic vesicles is tightly regulated and rapid, with fusion occurring within microseconds to milliseconds of Ca²⁺ influx. There are more than a dozen synaptotagmin family members in humans, which are expressed in neuronal cells and other cell types that regulate Ca²⁺-dependent exocytosis in different types of neurons (Cao *et al.*, 2013), mast cells (Melicoff *et al.*, 2009), and pancreatic β-cells (Gustavsson *et al.*, 2008). Fusion of endosomes and lysosomes is reportedly controlled by transient increases in Ca²⁺, with targets proposed to

findings suggest that SNARE-dependent fusion of ER-derived vesicles with Golgi membranes is distinct in sensitivity to changes in cytosolic calcium, at least in the 0.2–0.5 µM range.

Calcium signaling systems regulate major cellular processes, including exocytosis, cytoskeletal contraction, metabolism, gene transcription, and cellular proliferation. Transient changes in Ca^{2+} concentration can exert extremely rapid responses, whereas control of other processes occurs on the time scale of minutes to hours (Berridge et al., 2003). Our findings reveal that Ca^{2+} also influences ER–Golgi trafficking, although it remains an open question as to the cellular context in which this regulation might take place. Given that a twofold increase in cytosolic Ca^{2+} levels is sufficient to overcome complete loss of Ypt1 or Uso1 function, the fusion stage of ER–Golgi transport appears to be finely tuned to calcium concentrations. We propose that cytosolic Ca^{2+} levels could serve a global regulatory role to modulate transport rates through the early secretory pathway for coordination of membrane biogenesis with organelle size and growth rate. Indeed, a recent report indicates that elevated calcium levels in $pmr1\Delta$ strains stimulate vesicle trafficking to maintain organelle-specific divalent cation concentrations (Garcia-Rodriguez et al., 2015). In addition to Pmr1, multiple Ca^{2+} channels and pumps control cytosolic calcium levels in response to environmental status (D'Hooge et al., 2015). Overall regulation of intracellular Ca^{2+} homeostasis is complex and remains poorly understood, and dissection in model systems such as yeast should provide valuable insights.

MATERIALS AND METHODS

Yeast strains and media
Yeast strains used in this study are listed in Supplemental Table S1. All C-terminal epitope tagging was achieved using described methods (Longtine et al., 1998), and yeast transformations were performed using the lithium acetate technique (Ito et al., 1983). Deletion mutants containing the natMX4 cassette were generated with p4339 (Tong et al., 2001). Yeast cells were grown at 30°C (for wild-type strains) and 25°C (for mutant strains) in 1% yeast extract, 2% peptone, and 2% dextrose (YPD) medium unless otherwise noted. For plasmid selection, yeast cells were grown in 0.67% yeast nitrogen base and complete supplement with appropriate amino acid dropouts (MP Biomedicals, Solon, OH) and 2% dextrose (CSMD). Medium containing 5-FOA was prepared as described previously (Boeke et al., 1984). Bacterial strains DH5α and XL1-Blue were grown at 37°C in LB medium (1% NaCl, 1% Bacto-tryptone, and 0.5% Bacto-yeast extract) containing 100 µg/ml ampicillin if required. Growth assays in the presence of chelating agents were carried out in CSMD medium containing EGTA at a concentration of 5 mM or BAPTA at a concentration of 1.6 mM.

Plasmid construction
Plasmid pYEp511-SLY41 used in this study was described previously (Ossig et al., 1991). Construct pYEp511-SLY41ΔC was generated by mutagenesis of pYEp511-SLY41 to introduce stop codons into amino acid residues K447 and K448 using the QuikChange Site-Directed Mutagenesis Kit (Agilent, Santa Clara, CA). The plasmid pYX212-cytAEQ and conditions used to measure cytosolic calcium levels have been described previously (Buttner et al., 2013). All constructs were sequence verified by automated fluorescence sequencing (Dartmouth Molecular Biology Core Facility). Oligonucleotide primers used in this study are available upon request.

Antibodies and immunoblotting
Antibodies directed against Erv25 (Belden and Barlowe, 1996), Sec61 (Stirling et al., 1992), Kar2, Och1, Erv41, Erv46 (Otte et al.,

2001), Sec22 (Liu and Barlowe, 2002), and Erv26 (Bue et al., 2006) have been described previously. Polyclonal anti-Sly41 antiserum was raised against a glutathione-S-transferase (GST) fusion protein, GST-Sly41, containing amino acid residues 1–112 of the Sly41 predicted open reading frame. The GST-Sly41 fusion was expressed as a 39-kDa protein in DH5α cells and was contained in inclusion bodies that fractionated in the 14k pellet of cell lysates. Inclusion body pellets were washed with buffer containing 0.5% (vol/vol) Triton X-100 and resuspended in Tris-buffered saline buffer. The resuspended pellet was used to produce antiserum in rabbits (Covance, Denver, PA). The anti-Sly41 antiserum was typically used at a 1:1000 dilution for immunoblotting. Immunoblots were developed using Super Signal West Pico detection reagents (Thermo Scientific, Waltham, MA) and developed on both film and with a G:Box Bio-imaging system (Syngene, Frederick, MD).

Subcellular fractionation and sucrose velocity gradient sedimentation
ER (P13) and Golgi (P100) membrane fractions were collected by differential centrifugation of cell lysates prepared from wild-type and sec12-4 strains as described (Belden and Barlowe, 2001; Inadome et al., 2005) with minor modification. Cell cultures (25 ml) in logarithmic growth at 25°C were shifted to 38.5°C for 90 min to invoke temperature-sensitive blocks. Cells were harvested, resuspended in 4 ml of spheroplast buffer (0.7 M sorbitol, 10 mM Tris-Cl, pH 7.4, 0.5% glucose), treated with lytic enzyme, and chilled on ice, and spheroplasts were collected by centrifugation. Spheroplasts were resuspended in lysis buffer (0.1 M sorbitol, 50 mM KOAc, 2 mM EDTA, 20 mM 4-(2-hydroxyethyl)-1-piperazineethanesulfonic acid [HEPES], pH 7.5, 1 mM dithiothreitol, 1 mM phenylmethylsulfonyl fluoride [PMSF]) and lysed with a Dounce homogenizer at 4°C. Unlysed cells were cleared at 2500 × g for 10 min, and the supernatant fraction was centrifuged at 13,000 × g for 10 min to generate the P13 fraction. A P100 fraction was prepared from the P13 supernatant fluid after centrifugation at 100,000 × g for 15 min. Membrane pellets were resuspended in 50 µl of SDS–PAGE sample buffer, heated at 75°C for 5 min, and analyzed by immunoblot.

Velocity gradient sedimentation of membrane organelles was performed at 4°C (Powers and Barlowe, 1998) with minor modification. Spheroplasted cells were resuspended in lysis buffer (10 mM HEPES, pH 7.4, 12.5% sucrose, 1 mM EDTA, and 0.5 mM PMSF) and homogenized with 10 strokes of a Dounce homogenizer. The homogenates were centrifuged for 5 min at 4°C in an SS-34 rotor (Thermo Scientific) at 3500 rpm. The supernatant fraction was loaded onto the top of an 11-step sucrose step gradient (ranging from 18 to 60% sucrose in 10 mM HEPES, pH 7.5, and 1 mM $MgCl_2$). Gradients were centrifuged for 3 h at 36,000 rpm (SW40 rotor; Beckman Coulter, Indianapolis, IN). Fractions of 750 µl were taken from top to bottom and diluted 1:1 in SDS–PAGE sample buffer, and proteins were resolved on 10.5% polyacrylamide gels. Fractions were blotted for Sly41, Och1 (Golgi marker), and Sec61 (ER marker). Sucrose concentrations were measured by refractometry.

In vitro vesicle budding, tethering, and transport assays
Yeast semi-intact cell membranes from wild-type and mutant strains were prepared as described (Baker et al., 1988). Vesicle budding, tethering, and fusion assays using [^{35}S] gpαf were performed as described (Barlowe, 1997; Cao et al., 1998). Two-stage transport assays were performed (Cao and Barlowe, 2000) with vesicles isolated from wild-type microsomes and acceptor membranes prepared from both wild-type and Sly41-overexpressing semi-intact cells. Data points are the average of duplicate determinations, and the error bars represent

the range. To measure protein packaging into COPII vesicles, microsomes were prepared (Wuestehube and Schekman, 1992) and analytical-scale budding reactions performed (Otte *et al.*, 2001).

Indirect immunofluorescence microscopy

For indirect immunofluorescence microscopy as previously described (Powers and Barlowe, 1998), formaldehyde-fixed yeast cells were converted to spheroplasts and adhered to polylysine-coated slides. Cells were washed and incubated at room temperature in blocking buffer (1% bovine serum albumin and 0.5% Triton X-100 in phosphate-buffered saline) followed by development with primary antibodies. Polyclonal sera against Kar2 and Och1 were used at 1:300 and 1:200, respectively. For optimum detection, polyclonal serum against Sly41 was used at 1:50 in the wild-type and at 1:300 in the Sly41-overexpressor strain. Secondary fluorescein-conjugated anti-rabbit immunoglobulin G (Vector Laboratories, Burlingame, CA) was used at 1:200. Images were obtained at room temperature using a DeltaVision Imaging System (GE Healthcare, Pittsburgh, PA), comprising a customized inverted wide-field microscope (IX-71; Olympus), a UPlanS Apochromat 100×/1.40 numerical lens (Olympus, Center Valley, PA) with a CoolSNAP HQ2 camera (Photometrics, Tucson, AZ), and an Insight solid-state illumination unit. Images were processed by deconvolution in SoftWoRx (Applied Precision) and prepared with Photoshop (Adobe, San Jose, CA) and ImageJ (National Institutes of Health, Bethesda, MD).

Measurement of cytosolic free Ca^{2+} concentration

A pYX212-based plasmid containing a functional apoaequorin gene (pAEQ) was transformed into yeast using *URA3* gene as the selectable marker. This plasmid was a gift from Enzo Martegani (Department of Biotechnology and Biosciences, University of Milano-Bicocca, Milan, Italy). For analysis of basal cytosolic concentrations of Ca^{2+}, cells containing pYX212-cytAEQ were inoculated in CSMD (–Ura –Leu) at OD$_{600}$ = 0.1 and grown to mid log phase (OD$_{600}$ ≈ 1.0). Ten A_{600} units were harvested and processed as described previously (Miseta *et al.*, 1999). Luminometric analysis of the strains was carried out as kinetic (at 1-s intervals) and 20-s endpoint readings. An LMax II luminometer (Molecular Devices, Sunnyvale, CA) was used to collect aequorin light emission data. Data points are the average of triplicate determinations, and the error bars represent the range. The experiments were carried out three times independently, and a representative data set is presented in this study. The [Ca^{2+}]$_{cyt}$ values were derived from luminometric units using a previously described equation (Allen *et al.*, 1977).

Sample preparation for ICP-MS analysis

Yeast cultures were grown in the appropriate selective medium conditions to log phase, and 1 ml of culture was harvested at OD$_{600}$. = 1.The yeast cells were washed thrice with EDTA (1 µM, pH ~ 8), followed by three washes with deionized water. The yeast cells were acid digested (100 µl of nitric acid) at 75°C for 40 min. The digested yeast solutions were then diluted to a final volume of 500 µl with deionized water. The processed samples were analyzed using a 7700x Agilent ICP-MS (Trace Element Analysis Lab, Dartmouth College, Hanover, NH).

Oxidative cross-linking of cysteine-containing SNAREs

Disulfide cross-linking of SNAREs from semi-intact cells and two-stage transport reactions was performed as previously described (Flanagan *et al.*, 2015). Cross-linking of cysteine-containing SNAREs was induced by the addition of freshly prepared Cu(1,10-phenanthroline)$_2$SO$_4$ (Cu^{2+}/phen) to a final concentration of 200 µM

for 15 min. The reactions were quenched with 5× SDS–PAGE nonreducing sample buffer containing excess *N*-ethylmaleimide to quench any remaining free sulfhydryls. After heating and brief centrifugation to pellet-insoluble material, a portion of the sample was resolved by nonreducing SDS–PAGE and transferred to nitrocellulose, and filter-bound primary antibodies were detected on film by peroxidase-catalyzed chemiluminescence. Band intensities were quantified from films using the UN-SCAN-IT software package (Silk Scientific, Orem, UT).

REFERENCES

Allen DG, Blinks JR, Prendergast FG (1977). Aequorin luminescence: relation of light emission to calcium concentration—a calcium-independent component. Science 195, 996–998.

Antebi A, Fink GR (1992). The yeast Ca(2+)-ATPase homologue, PMR1, is required for normal Golgi function and localizes in a novel Golgi-like distribution. Mol Biol Cell 3, 633–654.

Baker D, Hicke L, Rexach M, Schleyer M, Schekman R (1988). Reconstitution of SEC gene product-dependent intercompartmental protein transport. Cell 54, 335–344.

Baker D, Wuestehube L, Schekman R, Botstein D, Segev N (1990). GTP-binding Ypt1 protein and Ca2+ function independently in a cell-free protein transport reaction. Proc Natl Acad Sci USA 87, 355–359.

Barlowe C (1997). Coupled ER to Golgi transport reconstituted with purified cytosolic proteins. J Cell Biol 139, 1097–1108.

Beckers CJ, Balch WE (1989). Calcium and GTP: essential components in vesicular trafficking between the endoplasmic reticulum and Golgi apparatus. J Cell Biol 108, 1245–1256.

Belden WJ, Barlowe C (1996). Erv25p, a component of COPII-coated vesicles, forms a complex with Emp24p that is required for efficient endoplasmic reticulum to Golgi transport. J Biol Chem 271, 26939–26946.

Belden WJ, Barlowe C (2001). Deletion of yeast p24 genes activates the unfolded protein response. Mol Biol Cell 12, 957–969.

Bentley M, Nycz DC, Joglekar A, Fertschai I, Malli R, Graier WF, Hay JC (2010). Vesicular calcium regulates coat retention, fusogenicity, and size of pre-Golgi intermediates. Mol Biol Cell 21, 1033–1046.

Berninsone P, Miret JJ, Hirschberg CB (1994). The Golgi guanosine diphosphatase is required for transport of GDP-mannose into the lumen of Saccharomyces cerevisiae Golgi vesicles. J Biol Chem 269, 207–211.

Berridge MJ, Bootman MD, Roderick HL (2003). Calcium signalling: dynamics, homeostasis and remodelling. Nat Rev Mol Cell Biol 4, 517–529.

Boeke JD, LaCroute F, Fink GR (1984). A positive selection for mutants lacking orotidine-5'-phosphate decarboxylase activity in yeast: 5-fluoro-orotic acid resistance. Mol Gen Genet 197, 345–346.

Brandizzi F, Barlowe C (2013). Organization of the ER-Golgi interface for membrane traffic control. Nat Rev Mol Cell Biol 14, 382–392.

Bue CA, Bentivoglio CM, Barlowe C (2006). Erv26p directs pro-alkaline phosphatase into endoplasmic reticulum–derived coat protein complex II transport vesicles. Mol Biol Cell 17, 4780–4789.

Buttner S, Faes L, Reichelt WN, Broeskamp F, Habernig L, Benke S, Kourtis N, Ruli D, Carmona-Gutierrez D, Eisenberg T, *et al.* (2013). The Ca2+/Mn2+ ion-pump PMR1 links elevation of cytosolic Ca(2+) levels to alpha-synuclein toxicity in Parkinson's disease models. Cell Death Differ 20, 465–477.

Caffaro CE, Hirschberg CB (2006). Nucleotide sugar transporters of the Golgi apparatus: from basic science to diseases. Acc Chem Res 39, 805–812.

Cao P, Yang X, Sudhof TC (2013). Complexin activates exocytosis of distinct secretory vesicles controlled by different synaptotagmins. J Neurosci 33, 1714–1727.

Cao Q, Zhong XZ, Zou Y, Murrell-Lagnado R, Zhu MX, Dong XP (2015). Calcium release through P2X4 activates calmodulin to promote endolysosomal membrane fusion. J Cell Biol 209, 879–894.

Cao X, Ballew N, Barlowe C (1998). Initial docking of ER-derived vesicles requires Uso1p and Ypt1p but is independent of SNARE proteins. EMBO J 17, 2156–2165.

Cao X, Barlowe C (2000). Asymmetric requirements for a Rab GTPase and SNARE proteins in fusion of COPII vesicles with acceptor membranes. J Cell Biol 149, 55–66.

Chen JL, Ahluwalia JP, Stamnes M (2002). Selective effects of calcium chelators on anterograde and retrograde protein transport in the cell. J Biol Chem 277, 35682–35687.

Colombo MI, Beron W, Stahl PD (1997). Calmodulin regulates endosome fusion. J Biol Chem 272, 7707–7712.

Cosson P, Letourneur F (1994). Coatomer interaction with di-lysine endoplasmic reticulum retention motifs. Science 263, 1629–1631.

Dascher C, Ossig R, Gallwitz D, Schmitt HD (1991). Identification and structure of four yeast genes (SLY) that are able to suppress the functional loss of YPT1, a member of the RAS superfamily. Mol Cell Biol 11, 872–885.

De Hertogh B, Carvajal E, Talla E, Dujon B, Baret P, Goffeau A (2002). Phylogenetic classification of transporters and other membrane proteins from Saccharomyces cerevisiae. Funct Integr Genomics 2, 154–170.

Demaegd D, Foulquier F, Colinet AS, Gremillon L, Legrand D, Mariot P, Peiter E, Van Schaftingen E, Matthijs G, Morsomme P (2013). Newly characterized Golgi-localized family of proteins is involved in calcium and pH homeostasis in yeast and human cells. Proc Natl Acad Sci USA 110, 6859–6864.

Demircioglu FE, Burkhardt P, Fasshauer D (2014). The SM protein Sly1 accelerates assembly of the ER-Golgi SNARE complex. Proc Natl Acad Sci USA 111, 13828–13833.

D'Hooge P, Coun C, Van Eyck V, Faes L, Ghillebert R, Marien L, Winderickx J, Callewaert G (2015). Ca(2+) homeostasis in the budding yeast Saccharomyces cerevisiae: impact of ER/Golgi Ca(2+) storage. Cell Calcium 58, 226–235.

Durr G, Strayle J, Plemper R, Elbs S, Klee SK, Catty P, Wolf DH, Rudolph HK (1998). The medial-Golgi ion pump Pmr1 supplies the yeast secretory pathway with Ca2+ and Mn2+ required for glycosylation, sorting, and endoplasmic reticulum-associated protein degradation. Mol Biol Cell 9, 1149–1162.

Feigenson GW (1986). On the nature of calcium ion binding between phosphatidylserine lamellae. Biochemistry 25, 5819–5825.

Flanagan JJ, Barlowe C (2006). Cysteine-disulfide cross-linking to monitor SNARE complex assembly during endoplasmic reticulum-Golgi transport. J Biol Chem 281, 2281–2288.

Flanagan JJ, Mukherjee I, Barlowe C (2015). Examination of Sec22 homodimer formation and role in SNARE-dependent membrane fusion. J Biol Chem 290, 10657–10666.

Gao XD, Kaigorodov V, Jigami Y (1999). YND1, a homologue of GDA1, encodes membrane-bound apyrase required for Golgi N- and O-glycosylation in Saccharomyces cerevisiae. J Biol Chem 274, 21450–21456.

Garcia-Rodriguez N, Manzano-Lopez J, Munoz-Bravo M, Fernandez-Garcia E, Muniz M, Wellinger RE (2015). Manganese redistribution by calcium-stimulated vesicle trafficking bypasses the need for P-type ATPase function. J Biol Chem 290, 9335–9347.

Gustavsson N, Lao Y, Maximov A, Chuang JC, Kostromina E, Repa JJ, Li C, Radda GK, Sudhof TC, Han W (2008). Impaired insulin secretion and glucose intolerance in synaptotagmin-7 null mutant mice. Proc Natl Acad Sci USA 105, 3992–3997.

Hadley B, Maggioni A, Ashikov A, Day CJ, Haselhorst T, Tiralongo J (2014). Structure and function of nucleotide sugar transporters: current progress. Comput Struct Biotechnol J 10, 23–32.

Halachmi D, Eilam Y (1996). Elevated cytosolic free Ca^{2+} concentrations and massive Ca^{2+} accumulation within vacuoles, in yeast mutant lacking PMR1, a homolog of Ca^{2+}-ATPase. FEBS Lett 392, 194–200.

Hardwick KG, Pelham HR (1992). SED5 encodes a 39-kD integral membrane protein required for vesicular transport between the ER and the Golgi complex. J Cell Biol 119, 513–521.

Hay JC (2007). Calcium: a fundamental regulator of intracellular membrane fusion. EMBO Rep 8, 236–240.

He L, Vasiliou K, Nebert DW (2009). Analysis and update of the human solute carrier (SLC) gene superfamily. Hum Genomics 3, 195–206.

Hediger MA, Romero MF, Peng JB, Rolfs A, Takanaga H, Bruford EA (2004). The ABCs of solute carriers: physiological, pathological and therapeutic implications of human membrane transport proteins. Introduction. Pflugers Arch 447, 465–468.

Heidtman M, Chen CZ, Collins RN, Barlowe C (2005). Yos1p is a novel subunit of the Yip1p-Yif1p complex and is required for transport between the endoplasmic reticulum and the Golgi complex. Mol Biol Cell 16, 1673–1683.

Helm JR, Bentley M, Thorsen KD, Wang T, Foltz L, Oorschot V, Klumperman J, Hay JC (2014). Apoptosis-linked gene-2 (ALG-2)/Sec31 interactions regulate endoplasmic reticulum (ER)-to-Golgi transport: a potential effector pathway for luminal calcium. J Biol Chem 289, 23609–23628.

Hoglund PJ, Nordstrom KJ, Schioth HB, Fredriksson R (2011). The solute carrier families have a remarkably long evolutionary history with the majority of the human families present before divergence of Bilaterian species. Mol Biol Evol 28, 1531–1541.

Huh WK, Falvo JV, Gerke LC, Carroll AS, Howson RW, Weissman JS, O'Shea EK (2003). Global analysis of protein localization in budding yeast. Nature 425, 686–691.

Inadome H, Noda Y, Adachi H, Yoda K (2005). Immunoisolaton of the yeast Golgi subcompartments and characterization of a novel membrane protein, Svp26, discovered in the Sed5-containing compartments. Mol Cell Biol 25, 7696–7710.

Ito H, Fukuda Y, Murata K, Kimura A (1983). Transformation of intact yeast cells treated with alkali cations. J Bacteriol 153, 163–168.

Jackson LP, Lewis M, Kent HM, Edeling MA, Evans PR, Duden R, Owen DJ (2012). Molecular basis for recognition of dilysine trafficking motifs by COPI. Dev Cell 23, 1255–1262.

Jensen LT, Ajua-Alemanji M, Culotta VC (2003). The Saccharomyces cerevisiae high affinity phosphate transporter encoded by PHO84 also functions in manganese homeostasis. J Biol Chem 278, 42036–42040.

Kito M, Seog DH, Igarashi K, Kambe-Honjo H, Yoda K, Yamasaki M (1996). Calcium and SLY genes suppress the temperature-sensitive secretion defect of Saccharomyces cerevisiae uso1 mutant. Biochem Biophys Res Commun 220, 653–657.

Lee MC, Miller EA, Goldberg J, Orci L, Schekman R (2004). Bi-directional protein transport between the ER and Golgi. Annu Rev Cell Dev Biol 20, 87–123.

Letourneur F, Gaynor EC, Hennecke S, Demolliere C, Duden R, Emr SD, Riezman H, Cosson P (1994). Coatomer is essential for retrieval of dilysine-tagged proteins to the endoplasmic reticulum. Cell 79, 1199–1207.

Lin SJ, Culotta VC (1996). Suppression of oxidative damage by Saccharomyces cerevisiae ATX2, which encodes a manganese-trafficking protein that localizes to Golgi-like vesicles. Mol Cell Biol 16, 6303–6312.

Liu Y, Barlowe C (2002). Analysis of Sec22p in endoplasmic reticulum/Golgi transport reveals cellular redundancy in SNARE protein function. Mol Biol Cell 13, 3314–3324.

Lobingier BT, Nickerson DP, Lo SY, Merz AJ (2014). SM proteins Sly1 and Vps33 co-assemble with Sec17 and SNARE complexes to oppose SNARE disassembly by Sec18. eLife 3, e02272.

Longtine MS, McKenzie A 3rd, Demarini DJ, Shah NG, Wach A, Brachat A, Philippsen P, Pringle JR (1998). Additional modules for versatile and economical PCR-based gene deletion and modification in Saccharomyces cerevisiae. Yeast 14, 953–961.

Mandal D, Woolf TB, Rao R (2000). Manganese selectivity of pmr1, the yeast secretory pathway ion pump, is defined by residue gln783 in transmembrane segment 6. Residue Asp778 is essential for cation transport. J Biol Chem 275, 23933–23938.

Mao Y, Du Y, Cang X, Wang J, Chen Z, Yang H, Jiang H (2013). Binding competition to the POPG lipid bilayer of Ca2+, Mg2+, Na+, and K+ in different ion mixtures and biological implication. J Phys Chem B 117, 850–858.

Margulis NG, Wilson JD, Bentivoglio CM, Dhungel N, Gitler AD, Barlowe C (2016). Analysis of COPII vesicles indicates a role for the Emp47-Ssp120 complex in transport of cell surface glycoproteins. Traffic 17, 191–210.

Martens S, McMahon HT (2008). Mechanisms of membrane fusion: disparate players and common principles. Nat Rev Mol Cell Biol 9, 543–556.

Melicoff E, Sansores-Garcia L, Gomez A, Moreira DC, Datta P, Thakur P, Petrova Y, Siddiqi T, Murthy JN, Dickey BF, et al. (2009). Synaptotagmin-2 controls regulated exocytosis but not other secretory responses of mast cells. J Biol Chem 284, 19445–19451.

Mi H, Muruganujan A, Thomas PD (2013). PANTHER in 2013: modeling the evolution of gene function, and other gene attributes, in the context of phylogenetic trees. Nucleic Acids Res 41, D377–386.

Micaroni M (2012). Calcium around the Golgi apparatus: implications for intracellular membrane trafficking. Adv Exp Med Biol 740, 439–460.

Miseta A, Kellermayer R, Aiello DP, Fu L, Bedwell DM (1999). The vacuolar Ca2+/H+ exchanger Vcx1p/Hum1p tightly controls cytosolic Ca2+ levels in S. cerevisiae. FEBS Lett 451, 132–136.

Nakajima H, Hirata A, Ogawa Y, Yonehara T, Yoda K, Yamasaki M (1991). A cytoskeleton-related gene, uso1, is required for intracellular protein transport in Saccharomyces cerevisiae. J Cell Biol 113, 245–260.

Newman AP, Shim J, Ferro-Novick S (1990). BET1, BOS1, and SEC22 are members of a group of interacting yeast genes required for transport from the endoplasmic reticulum to the Golgi complex. Mol Cell Biol 10, 3405–3414.

Orlean P (2012). Architecture and biosynthesis of the Saccharomyces cerevisiae cell wall. Genetics 192, 775–818.

Ossig R, Dascher C, Trepte HH, Schmitt HD, Gallwitz D (1991). The yeast SLY gene products, suppressors of defects in the essential GTP-binding Ypt1 protein, may act in endoplasmic reticulum-to-Golgi transport. Mol Cell Biol 11, 2980–2993.

Otte S, Barlowe C (2002). The Erv41p-Erv46p complex: multiple export signals are required in trans for COPII-dependent transport from the ER. EMBO J 21, 6095–6104.

Otte S, Belden WJ, Heidtman M, Liu J, Jensen ON, Barlowe C (2001). Erv41p and Erv46p: new components of COPII vesicles involved in transport between the ER and Golgi complex. J Cell Biol 152, 503–518.

Parkinson K, Baines AE, Keller T, Gruenheit N, Bragg L, North RA, Thompson CR (2014). Calcium-dependent regulation of Rab activation and vesicle fusion by an intracellular P2X ion channel. Nat Cell Biol 16, 87–98.

Parlati F, McNew JA, Fukuda R, Miller R, Sollner TH, Rothman JE (2000). Topological restriction of SNARE-dependent membrane fusion. Nature 407, 194–198.

Pedersen UR, Leidy C, Westh P, Peters GH (2006). The effect of calcium on the properties of charged phospholipid bilayers. Biochim Biophys Acta 1758, 573–582.

Peng R, Gallwitz D (2002). Sly1 protein bound to Golgi syntaxin Sed5p allows assembly and contributes to specificity of SNARE fusion complexes. J Cell Biol 157, 645–655.

Peters C, Mayer A (1998). Ca2+/calmodulin signals the completion of docking and triggers a late step of vacuole fusion. Nature 396, 575–580.

Porat A, Elazar Z (2000). Regulation of intra-Golgi membrane transport by calcium. J Biol Chem 275, 29233–29237.

Portnoy ME, Liu XF, Culotta VC (2000). Saccharomyces cerevisiae expresses three functionally distinct homologues of the nramp family of metal transporters. Mol Cell Biol 20, 7893–7902.

Powers J, Barlowe C (1998). Transport of axl2p depends on erv14p, an ER-vesicle protein related to the Drosophila cornichon gene product. J Cell Biol 142, 1209–1222.

Rexach MF, Schekman RW (1991). Distinct biochemical requirements for the budding, targeting, and fusion of ER-derived transport vesicles. J Cell Biol 114, 219–229.

Romero PA, Herscovics A (1989). Glycoprotein biosynthesis in Saccharomyces cerevisiae. Characterization of alpha-1,6-mannosyltransferase which initiates outer chain formation. J Biol Chem 264, 1946–1950.

Rudolph HK, Antebi A, Fink GR, Buckley CM, Dorman TE, LeVitre J, Davidow LS, Mao JI, Moir DT (1989). The yeast secretory pathway is perturbed by mutations in PMR1, a member of a Ca2+ ATPase family. Cell 58, 133–145.

Sacher M, Barrowman J, Wang W, Horecka J, Zhang Y, Pypaert M, Ferro-Novick S (2001). TRAPP I implicated in the specificity of tethering in ER-to-Golgi transport. Mol Cell 7, 433–442.

Sapperstein SK, Lupashin VV, Schmitt HD, Waters MG (1996). Assembly of the ER to Golgi SNARE complex requires Uso1p. J Cell Biol 132, 755–767.

Schindler R, Itin C, Zerial M, Lottspeich F, Hauri HP (1993). ERGIC-53, a membrane protein of the ER-Golgi intermediate compartment, carries an ER retention motif. Eur J Cell Biol 61, 1–9.

Schmitt HD, Puzicha M, Gallwitz D (1988). Study of a temperature-sensitive mutant of the ras-related YPT1 gene product in yeast suggests a role in the regulation of intracellular calcium. Cell 53, 635–647.

Schröder S, Schimmoller F, Singer-Kruger B, Riezman H (1995). The Golgi-localization of yeast Emp47p depends on its di-lysine motif but is not affected by the ret1-1 mutation in alpha-COP. J Cell Biol 131, 895–912.

Segev N, Mulholland J, Botstein D (1988). The yeast GTP-binding YPT1 protein and a mammalian counterpart are associated with the secretion machinery. Cell 52, 915–924.

Simunovic M, Lee KY, Bassereau P (2015). Celebrating Soft Matter's 10th anniversary: screening of the calcium-induced spontaneous curvature of lipid membranes. Soft Matter 11, 5030–5036.

Sogaard M, Tani K, Ye RR, Geromanos S, Tempst P, Kirchhausen T, Rothman JE, Sollner T (1994). A rab protein is required for the assembly of SNARE complexes in the docking of transport vesicles. Cell 78, 937–948.

Stirling CJ, Rothblatt J, Hosobuchi M, Deshaies R, Schekman R (1992). Protein translocation mutants defective in the insertion of integral membrane proteins into the endoplasmic reticulum. Mol Biol Cell 3, 129–142.

Sudhof TC (2013). Neurotransmitter release: the last millisecond in the life of a synaptic vesicle. Neuron 80, 675–690.

Tarafdar PK, Chakraborty H, Dennison SM, Lentz BR (2012). Phosphatidyl-serine inhibits and calcium promotes model membrane fusion. Biophys J 103, 1880–1889.

Teasdale RD, Jackson MR (1996). Signal-mediated sorting of membrane proteins between the endoplasmic reticulum and the golgi apparatus. Annu Rev Cell Dev Biol 12, 27–54.

Tong AH, Evangelista M, Parsons AB, Xu H, Bader GD, Page N, Robinson M, Raghibizadeh S, Hogue CW, Bussey H, et al. (2001). Systematic genetic analysis with ordered arrays of yeast deletion mutants. Science 294, 2364–2368.

von Heijne G (1992). Membrane protein structure prediction. Hydrophobicity analysis and the positive-inside rule. J Mol Biol 225, 487–494.

Wuestehube LJ, Schekman RW (1992). Reconstitution of transport from endoplasmic reticulum to Golgi complex using endoplasmic reticulum-enriched membrane fraction from yeast. Methods Enzymol 219, 124–136.

Yaghmur A, Sartori B, Rappolt M (2011). The role of calcium in membrane condensation and spontaneous curvature variations in model lipidic systems. Phys Chem Chem Phys 13, 3115–3125.

Yanagisawa K, Resnick D, Abeijon C, Robbins PW, Hirschberg CB (1990). A guanosine diphosphatase enriched in Golgi vesicles of Saccharomyces cerevisiae. Purification and characterization. J Biol Chem 265, 19351–19355.